Atmos. Chem. Phys. Discuss., 11, 20521–20573, 2011
www.atmos-chem-phys-discuss.net/11/20521/2011/
doi:10.5194/acpd-11-20521-2011

Atmospheric Chemistry and Physics Discussions

Ionic and carbonaceous compositions of PM_{10}, $PM_{2.5}$ and $PM_{1.0}$ at Gosan ABC superstation and their ratios as source signature

S. Lim[1,*], M. Lee[1], G. Lee[2], S. Kim[3], S. Yoon[3], and K. Kang[4]

[1]Dep. of Earth and Environmental Sciences, Korea University, Seoul, South Korea
[2]Dep. of Environmental Science, Hankuk University of Foreign Studies, Seoul, South Korea
[3]School of Earth and Environmental Sciences, Seoul National University, Seoul, South Korea
[4]Graduate program in Marine Meteorology, Jeju National University, Jeju, South Korea
[*]now at: Laboratoire de Glaciologie et Géophysique de l'Environnement (LGGE), CNRS/University of Grenoble, Grenoble, France

Received: 26 April 2011 – Accepted: 15 June 2011 – Published: 19 July 2011

Correspondence to: M. Lee (meehye@korea.ac.kr)

Published by Copernicus Publications on behalf of the European Geosciences Union.

Abstract

$PM_{1.0}$, $PM_{2.5}$, and PM_{10} were sampled at Gosan ABC Superstation on Jeju Island from August 2007 to September 2008. The carbonaceous aerosols were quantified with the thermal/optical reflectance (TOR) method, which produced five organic carbon (OC) fractions, OC1, OC2, OC3, OC4, and pyrolyzed organic carbon (OP), and three elemental carbon (EC) fractions, EC1, EC2, and EC3. The mean mass concentrations of $PM_{1.0}$, $PM_{2.5}$, and PM_{10} were 13.72 $\mu g\,m^{-3}$, 17.24 $\mu g\,m^{-3}$, and 28.37 $\mu g\,m^{-3}$, respectively. The averaged mass fractions of OC and EC were 23.0 % and 10.4 % for $PM_{1.0}$, 22.9 % and 9.8 % for $PM_{2.5}$, and 16.4 % and 6.0 % for PM_{10}. Among the OC and EC sub-components, OC2 and EC2+3 were enriched in the fine mode, but OC3 and OC4 in the coarse mode. The filter-based $PM_{1.0}$ EC agreed well with black carbon (BC) measured by an Aethalometer, and PM_{10} EC was higher than BC, implying less light absorption by larger particles. EC was well correlated with sulfate, resulting in good relationships of sulfate with both aerosol scattering coefficient measured by Nephelometer and BC concentration. Our measurements of EC confirmed the definition of EC1 as char-EC emitted from smoldering combustion and EC2+3 as soot-EC generated from higher-temperature combustion such as motor vehicle exhaust and coal combustion. In particular, EC1 was strongly correlated with potassium, a traditional biomass burning indicator, except during the summer, when the ratio of EC1 to EC2+3 was the lowest. We also found the ratios of major chemical species to be a useful tool to constrain the main sources of aerosols, by which the five air masses were well distinguished: Siberia, Beijing, Shanghai, Yellow Sea, and East Sea types. Except Siberian air, the continental background of the study region, Beijing plumes showed the highest EC1 (and OP) to sulfate ratio, which implies that this air mass had the highest net warming by aerosols of the four air masses. Shanghai-type air, which was heavily influenced by southern China, showed the highest sulfate enhancement. The highest EC2+3/EC1 ratio was found in aged East Sea air, demonstrating a significant influence of motor vehicle emissions from South Korea and Japan and less influence from industrial regions

ACPD

11, 20521–20573, 2011

of China. The high ratio results from the longer residence time and less sensitivity to wet scavenging of EC2+3 compared to EC1, indicating that soot-EC could have greater consequence in regional-scale warming.

1 Introduction

Atmospheric aerosols play an important role in climate change by influencing the global radiation balance both directly and indirectly. The direct effect is the mechanism by which aerosols scatter and absorb shortwave and longwave radiation, thereby altering the radiative balance of the Earth-atmosphere system (IPCC, 2007). The relative importance of these processes depends on the chemical composition and size distribution of aerosols (Ramachandran, 2009). Aerosols also cause a negative radiative forcing indirectly through changes in cloud properties. This indirect effect includes the role of aerosols in modifying cloud droplet number concentration and cloud lifetime (IPCC, 2007; Haywood and Boucher, 2000).

Because the chemical composition and size distribution of aerosols are important in quantifying their radiative effects (Brasseur et al., 1999; Ramanathan et al., 2001; Buzorius et al., 2004), knowledge of the chemical composition of atmospheric aerosols of a given size is required to assess their impact on the environment. Aerosols are often classified into submicron and supermicron particles; the former are of particular concern to public health and climate change because they mainly originate from anthropogenic sources and interact more efficiently with sunlight. Anthropogenic sources contribute almost as much as natural sources to the global aerosol optical depth (AOD) (Hansen et al., 1997; Robertson et al., 2001). Anthropogenic aerosols are typically composed of various inorganic and organic species (IPCC, 2007), among which sulfate, nitrate, and carbonaceous aerosols including black carbon (BC) and organic carbon (OC) are of major interest due to their atmospheric abundances. In particular, carbonaceous aerosols are major contributors to fine aerosols smaller than 1 and typically constitute a significant, sometimes dominant, fraction of the total fine particle mass of submicron particles (Gray et al., 1986; Shah et al., 1986; Andrews et al.,

ACPD
11, 20521–20573, 2011

2000; Yang et al., 2005). They are composed of light-absorbing carbon as well as light-scattering carbon. The radiative forcing at the top of the atmosphere is found to change sign from negative to positive when carbonaceous aerosols are abundant over highly reflecting surfaces such as land and snow, which results in higher atmospheric heating (Ramanathan and Carmichael, 2008; Ramachandran, 2009).

These carbonaceous aerosols are mainly divided into two categories: elemental carbon (EC), often called BC or soot, and OC. Especially for EC, there are various definitions and analytical methods to quantify its atmospheric concentration (Andreae and Gelensér, 2006; Han et al., 2010). EC is usually referred to a near-elemental soot-carbon-like composition and to the fraction of carbon that is oxidized in combustion analysis above a certain temperature threshold. Soot carbon may be defined as aggregates of spherules made of grapheme layers, consisting almost purely of carbon, with minor amounts of bound heteroelements, especially hydrogen and oxygen, whereas soot is referred to a black, blackish or brown substance formed by combustion, present in the atmosphere as fine particles. BC generally implies to have optical properties and composition similar to soot carbon (Andreae and Gelensér, 2006). While EC is usually determined by thermal methods based on its chemical properties, BC is measured using its optical properties. Therefore, BC is considered as light-absorbing EC and is generally lower in concentration than EC. EC enters the atmosphere exclusively as a primary (i.e., direct particulate) emission originating nearly completely from pyrolysis during incomplete combustion, mainly of biomass and fossil fuel (Nunes and Pio, 1993; Bond et al., 2007). Because EC is optically absorptive and highly polyaromatic, it has recently been a subject of interest in many studies encompassing local to global scales. In particular, EC (or BC) could be the next most important contributor to global warming, in terms of direct forcing, after CO_2 (Kuhlbusch and Crutzen, 1995; Jacobson, 2001; Oen et al., 2006; Ramanathan and Xu, 2010). The surface forcing is about 2–3 times larger than the forcing at the top of the atmosphere for absorbing aerosols such as EC, producing a large atmospheric warming (Ramanathan and Carmichael, 2008).

ACPD
11, 20521–20573, 2011

On the other hand, OC is commonly considered as the non-absorptive fraction of the carbonaceous aerosol. It has more molecular forms and a lower molecular weight than EC. OC is produced from both direct emission and gaseous precursors by atmospheric oxidation or oligomerization (Jacobson et al., 2000; Kanakidou et al., 2005; Tsigaridis et al., 2006). The main primary source of OC is combustion along with EC emissions and biogenic emissions. In addition, OC is produced from oxidation of precursor gases in the atmosphere, constituting what is called secondary organic aerosol (SOA) (Jacobson et al., 2000). A considerable proportion of organic aerosols is hygroscopic, thereby serving as cloud condensation nuclei (CCN) along with sulfate aerosols. On the other hand, EC particles are hydrophobic when they are emitted, but the sulfates or water soluble organic compounds (WSOC) that become attached to EC particles can change them from hydrophobic to hydrophilic, eventually making them efficient CCN (Decesari et al., 2002; Persiantseva et al., 2004; Petzold et al., 2005). When EC was coated with reflecting compounds like OC, the absorption by EC was found to increase at least by a factor of 1.5 (Bond et al., 2006). In addition, carbonaceous aerosols, when mixed with atmospheric dust, have the potential to influence the atmospheric chemistry of several trace gases such as NO_2, O_3, and SO_2 (Dentener et al., 1996).

Although the definition and measurement techniques for atmospheric EC or BC have long been subjects of scientific controversy, the recent discovery of light-absorbing carbon that is not black but brown (or yellowish) makes it imperative to reassess and redefine the components that make up light-absorbing carbonaceous matter in the atmosphere (Andreae and Gelencsér, 2006). There has been growing evidence for the contribution of brown carbon to light absorption in atmospheric aerosols from chemical aerosol measurements and laboratory studies (Mukai and Ambe, 1986; Havers et al., 1998; Hoffer et al., 2006; Alexander et al., 2008; Park et al., 2010).

Unlike the principal greenhouse gases, aerosols are more concentrated in the source regions and exhibit strong spatial and temporal variations. Furthermore, they have an impact on global climate because their radiative influence can be transported due to changes in the mean atmospheric circulation patterns (Ramachandran, 2009).

ACPD
11, 20521–20573, 2011

Therefore, finding a source and a source region of major components of aerosols, such as carbonaceous species, sulfate, and nitrate, is crucial for the assessment of their radiative effect. In particular, Asia is the main source of global anthropogenic aerosol emission. At present, anthropogenic emissions of gaseous pollutants in Asia are larger than those in Europe and North America and will continue to increase in the future (Akimoto, 2003). An emission inventory study in Asia suggests that 30–60 % of the total emission of aerosol gaseous precursors and primary BC and OC are emitted in China. In particular, ~41 % of submicron BC emissions is originated in China (Streets et al., 2003). The recently documented linear increase of primary BC and OC between 1850 and 2000 highlights the importance of continuous measurements of carbonaceous particles (Bond et al., 2007). Additionally, the frequent presence of desert dust makes the East Asian atmosphere more complex because of both scattering of sunlight and absorption of radiation (Hubert et al., 2003).

In recent decades, carbonaceous aerosols, both EC and OC, have been measured in many regions of Northeast Asia, including South Korea, China, and Japan (Ohta et al., 1998; Kim et al., 2000; Park et al., 2001; Cao et al., 2005; Hagler et al., 2006; Lee et al., 2007, 2008, 2009; Shen et al., 2007; Moon et al., 2008; Aggarwal and Kawamura, 2009). The areas covered have included urban areas (Park et al., 2001; Lee et al., 2009), developing regions (Hagler, 2006), and sandlands (Cao et al., 2005; Shen et al., 2007). However, most of these studies focused on $PM_{2.5}$ or PM_{10} and were conducted during a specific season, such as spring (Lee et al., 2007; Shen et al., 2007), spring and early summer (Aggarwal and Kawamura, 2009), or fall and winter (Cao et al., 2005). There have been few year-round studies of both fine and coarse aerosols, particularly at a site where it is feasible to monitor long-range transport and the atmospheric processes involving air pollutants emitted from the Asian continent. This limitation hinders the full characterization of carbonaceous aerosols in Northeast Asia.

ACPD
11, 20521–20573, 2011

In the present study, we measured soluble ionic and carbonaceous compositions of $PM_{1.0}$, $PM_{2.5}$, and PM_{10}at Gosan ABC Superstation on Jeju Island throughout the year from August 2007 to September 2008. The main objective was threefold: to understand distributions and behavior of major components, particularly carbonaceous components, of both fine and coarse aerosols; to identify the sources of these components; and finally to examine the relationships between chemical compositions and optical properties.

2 Measurement

$PM_{1.0}$, $PM_{2.5}$, and PM_{10} were measured at Gosan ABC Superstation on Jeju Island during August 2007–September 2008. Gosan station (33.17° N, 126.10° E, 70 m a.s.l., Fig. 1) served as a base for the ACE-Asia experiment in 2001 and was designated as one of the ABC Superstations (Lee et al., 2007). It has been considered to be an ideal location to monitor Asian outflows and assess their impact on air quality over the northern Pacific (Carmichael et al., 1996, 1997; Chen et al., 1997).

In the present study, the concentrations of water-soluble inorganic ions, EC, OC, and mass in $PM_{1.0}$, $PM_{2.5,}$ and PM_{10} were measured for about one year. Ambient air was collected through $PM_{1.0}$, $PM_{2.5,}$ and PM_{10} sharp-cut cyclone coated with Teflon (URG, USA) at 16.7 LPM, and cumulative flow was measured with a dry gas-meter. These low-volume samplers were installed at the top of a 10-m tower. Particles were collected on pre-weighed 37-mm Teflon filters for mass and ion analysis, and on pre-heated 37-mm quartz-fiber filters (Pall corp., USA) for carbon analysis.

Sampling was conducted usually once every six days. It started at 0900 LST and lasted for 24 h. There was less number of samples collected during summer and winter monsoon periods because of rain, snow, or strong wind. With additional samples during particular events such as Asian dust and pollution plumes, a total of 41 sets of samples were taken for this study (Table 1).

ACPD
11, 20521–20573, 2011

Eight species of water-soluble ions, which included SO_4^{2-}, NO_3^-, Cl^-, NH_4^+, K^+, Na^+, Ca^{2+}, and Mg^{2+}, were determined by ion chromatography (Dionex 4500, Dionex, USA). More details on this method of analysis can be found in Lim (2009). EC, OC, and TC were analyzed at the Desert Research Institute (Reno, NV, USA) following the Interagency Monitoring of Protected Visual Environments (IMPROVE) thermal/optical reflectance protocol. Thermal/optical methods assume EC is a low-volatility carbon fraction that is not liberated in an oxygen-free environment until a temperature of >600° is attained, allowing it to be separated from the more volatile OC that evolves at lower temperatures. Eight fractions of carbon, including four fractions of OC (at 120° for OC1, at 250° for OC2, at 450° for OC3, and at 550° for OC4 in a He atmosphere), three fractions of EC (at 550° for EC1, at 700 ° for EC2, and at 800° for EC3 in a 2 % O_2/98 % He atmosphere), and OP, pyrolyzed (or charred) OC, were determined by this analysis method. OP is measured after the introduction of a He/O_2 atmosphere but before reflectance or transmittance returns to its initial value (Chow et al., 2005).

In conjunction with chemical composition, BC concentration was determined by absorption at 7 wavelengths, 370, 450, 520, 590, 660, 880, and 950 nm, using an Aethalometer (AE-31, Magee Scientific Corp., USA) every 10 min. Scattering coefficients were obtained at 450 nm, 550 nm, and 700 nm by a Nephelometer (model 3563, TSI Inc., USA) every 10 min. For these measurements, ambient air was pulled through a sampling manifold without cut-points. These optical measurement data are available since January 2008. Gaseous pollutants, including O_3, NO_2, CO, and SO_2, and a meteorological suite were measured hourly by the National Institute of Environmental Research (NIER) and the Korea Meteorological Administration (KMA), respectively. These data were averaged hourly or daily for comparison with the chemical composition data.

ACPD
11, 20521–20573, 2011

3 Size-fractionated ionic and carbonaceous compositions

The daily concentrations of $PM_{1.0}$, $PM_{2.5}$, and PM_{10} varied between 1.26 $\mu g\,m^{-3}$ and 29.51 $\mu g\,m^{-3}$, 3.94 $\mu g\,m^{-3}$ and 39.17 $\mu g\,m^{-3}$, and 7.52 $\mu g\,m^{-3}$ and 69.7 $\mu g\,m^{-3}$, respectively. Mean mass concentrations were 13.72 $\mu g\,m^{-3}$ for $PM_{1.0}$, 17.24 $\mu g\,m^{-3}$ for $PM_{2.5}$, and 28.37 $\mu g\,m^{-3}$ for PM_{10} (Fig. 2 and Table 2), suggesting that the daily mass well represented episodic events associated with pollution and dust plumes. Caution needs to be exerted when comparing these values with annual mean because there is relatively less number of samples during summer and winter monsoon periods. The noticeable feature was a large fraction of $PM_{1.0}$ against PM_{10}(48.4 %) and against $PM_{2.5}$ (60.8 %) on average. $PM_{2.5}$ accounted for 79.6 % of PM_{10}.

In particulate matter of all sizes, the most abundant constituents were water-soluble ions, which were followed by OC and EC (Fig. 2). We did not convert OC to OM, and the following discussion is pertinent only to OC. The concentrations of ions were almost twice as high as those of OC, and OC was nearly two times higher than EC. The average mass fractions of ions, OC, and EC were 53.9 %, 23.0 %, and 10.4 % for $PM_{1.0}$, 52.4 %, 22.9 %, and 9.8 % for $PM_{2.5}$, and 43.4 %, 16.4 %, and 6.0 % for PM_{10}, revealing that carbonaceous compounds were the most abundant in $PM_{1.0}$ and $PM_{2.5}$. A considerable fraction of mass other than water-soluble ions, OC, and EC was possibly due to trace metals and silica, which were not measured.

The ratios of OC/EC were 2.2, 2.3, and 2.8 for $PM_{1.0}$, $PM_{2.5}$, and PM_{10}, respectively. These mean OC/EC ratios were much lower than those measured at the regional background (RB) site in Western Mediterranean (~11 for $PM_{2.5}$) (Pey et al., 2009) and at two RB sites in western China (~12 for PM_{10}) (Qu et al., 2009), and still lower than those of most RB sites in Europe (OC/EC > 4) (Pey et al., 2009). The difference in OC/EC ratios is likely due to relatively higher EC concentration than OC in this study area. Our OC/EC ratios were, however, comparable to those for $PM_{2.5}$ (2.4) and PM_{10} (2.5) in Pearl River Delta Region (PRDR), China during winter period (Cao et al., 2003).

ACPD
11, 20521–20573, 2011

The distributions of TC/mass, OC/mass, and EC/mass among particle sizes were very similar, increasing with decrease in particle diameter (Fig. 3a, b, and c). The trends imply substantial anthropogenic influence and atmospheric processing such as condensation, gas-to-particle conversion, or surface-limited oxidation processes. For fine mode OC, there could be contribution from biogenic emissions as well as anthropogenic sources. Additionally, EC/mass distributions were slightly sharper than OC/mass with decrease in particle size, indicating a larger contribution of EC to fine particles. For water-soluble ions, sulfate was the most abundant single species, and its concentration was comparable to that of TC, accounting for 20 ~ 30 % of the mass (Fig. 3e). Also, the sulfate-to-mass ratio was found to be slightly more shifted toward $PM_{1.0}$ than was the TC-to-mass ratio, while being similar in size distribution. This shift is probably due to a large amount of non-sea-salt sulfate (nss-SO_4^{2-}) originating from anthropogenic sources, which contributed about ~ 75–99 % of total sulfate aerosols, and is dependent on gas-to-particle conversion processes. The concentrations of nss components were calculated from the measured sodium concentrations and the ratio of the component to sodium in seawater.

In contrast to the carbonaceous aerosols and the sulfate, significant differences in size distributions were observed for calcium and nitrate (Fig. 3d and f). These species were much higher in PM_{10} than in the other size fractions. In the case of nitrate, the next most abundant species among the water-soluble ions, this is due to its chemical and physical characteristics, especially its volatility. Nitrate, being more volatile than sulfate, will tend to evaporate from smaller particles and deposit on large particles, where surface curvature effects on vapor pressure are minimal, while sulfate, being essentially non-volatile, has a size distribution controlled by gas-phase diffusion and will tend to accumulate in small particles (Bassett and Seinfeld, 1984). For calcium, its main sources are soils and sea salt in general; however, the soil-derived calcium would be a more abundant component of total calcium in the present study because non-sea-salt-calcium (nss-Ca^{2+}) accounts for ~43–97 % of the total calcium in all particle sizes. In previous studies, it has been suggested that nitrate is formed through

ACPD
11, 20521–20573, 2011

heterogeneous reactions including nitrogen oxides and by absorption of nitric acid on the surface of soil particles (Mamane and Gottlieb, 1989; Zhang et al., 1994). At the Gosan station, the correlation between nitrate and calcium in PM_{10} was significant ($R^2 = 0.51$) for all measurements, including the high PM_{10} episodes that were affected by Asian dust event. The correlation implies that there is a mineral affinity of nitrate in coarse mode particles and that some of the nitrate could have been formed on dust particles enriched with calcium. In fact, there have been intensive studies on the link between anthropogenic nitrate or sulfate and mineral constituents of Asian dust (Wang et al., 2007; Lin et al., 2008; Geng et al., 2009) and Saharan dust particles (Talbot et al., 1986; Mace et al., 2003; Koçak et al., 2004). Particularly, Geng et al. (2009) reported that the nitrate-containing secondary soil-derived particles were markedly increased in coarse mode during Asian dust period. Asian dust was also suggested to provide a removal mechanism for NO_x (or HNO_3) and perhaps contribute to nitrogen deposition in the Yellow Sea (Wu and Okada, 1994).

The ratios of OC and EC to TC as a function of particle diameter (Fig. 3g and h) reflect the oxidation and condensation mechanisms of carbonaceous compounds. Gas-to-particle conversion and heterogeneous chemistry in the atmosphere control chemical and physical properties of aerosols, but these processes are not understood well enough to predict accurately the evolution of the gas and particle-phase composition of the troposphere (Ravishankara, 1997; Maria et al., 2004). In particular, the formation and the mixing state of carbonaceous aerosols are important due to their considerable anthropogenic source and high concentration. As shown in Figures 3g and 3h, the EC-to-TC ratio increased with decrease in particle size, while the OC-to-TC ratio showed an opposite trend. Particles generated through condensation of hot vapor or from direct emissions can become oxidized through heterogeneous reactions that are surface-limited or volume-limited (Worsnop et al., 2002). EC particles were likely controlled by surface-limited processes in the study region because the localization of the reactions at the particle surfaces results in larger concentrations of carbon in smaller aerosol particles with larger surface-to-volume ratios than larger particles (Maria et al.,

ACPD
11, 20521–20573, 2011

2004). Although EC is mixed with organic compounds in the atmosphere, surface-limited oxidation may easily occur because organic compounds often have efficient surface reactivity (Maria et al., 2004; Russell et al., 2002). In the case of OC, interestingly, the OC/TC ratio was highest in the coarse mode and lowest in $PM_{1.0}$. The OC enrichment in coarse mode could be attributed to the formation of secondary organic aerosols (SOA) and subsequent increase in size during aging processes (Liu et al., 2009). The relatively higher OC/EC ratio (2.5 for $PM_{2.5}$ and 3.3 for PM_{10}) in spring and summer implies SOA formation at higher temperature, even though OC concentrations were lower than those in winter. Mochida et al. (2007) performed size-segregated aerosol measurements off the coast of East Asia and found a high OC proportion in the supermicron mode of up to 61 %, suggesting primary emission of organics associated with sea salt and dust particles or other primary sources (e.g., plant waxes, soil-derived microbes, and anthropogenic particles). In this measurement, a similar behavior of OC and EC was observed during an Asian dust event in May 2008 (Lim et al., 2010), in which the ratio of OC to EC was raised in dust-laden air possibly due to the impact of dust-related primary OC. Therefore, it is suggested that there was a considerable contribution of primary OC as well as SOA to total OC concentration particularly in the present study.

The ratios of OC and EC subcomponents to TC (Fig. 3i–o) were divided into three types. The first group includes OC1, OP, and EC1, whose ratios against TC did not show a clear tendency to vary with particle size (Fig. 3i, m, and n). OC1 may represent semi-volatile organic carbon because OC1 not only is the first carbon evolved at the lowest temperature but also is observed to be the most abundant and variable in concentration among the 5 OC fractions in our blank filters. OP is a measure of pyrolyzed organic carbon, and its characteristics are well described by Andreae and Gelencsér (2006), who explained that OP can be released as a gas or in solid form and become associated with submicron or supermicron particles. Similarly, EC1 was defined as charred EC (Han et al., 2010), and a detailed discussion of EC1 is given in Sect. 5. The second group includes OC2 and EC2+3, whose ratios to TC were enhanced in

ACPD
11, 20521–20573, 2011

the smaller size particles (Fig. 3j and o). This enhancement strongly supports the view that a condensation process or surface-limited oxidation was involved in the formation of OC2 and EC2+3. Particularly, OC2 is thought to be a secondary organic carbon, which will be further discussed in Sect. 6. In contrast to OC2, the fractions OC3 and OC4 clearly increased with increasing particle size (Fig. 3k and l), and their concentrations were also higher in PM_{10} than in $PM_{1.0}$, suggesting the characteristic of primary aerosols.

4 Seasonal characteristics

The monthly variations of meteorological parameters include those of temperature, which varied between 4.4 °C and 25.8 °C, and relative humidity, which ranged from 37.2 % to 87.6 % over the whole period, showing distinct seasonal patterns. The mode of wind direction in degrees from 0° to 360° was chosen for each month and categorized into eight groups from N to NW. Throughout the winter and the spring, the prevailing wind was northwesterly under the influence of the winter monsoon over East Asia, with high wind speeds up to 13 $m\,s^{-1}$, suggesting a greater influence during that period from Asian continental outflows. With the arrival of summer, the wind direction was shifted to easterly with lower wind speeds below 3 $m\,s^{-1}$, indicating reduced continental outflows (Kim et al., 2007).

Seasonal mass fractions of major components (OC, EC, nitrate, and, sulfate) and mass concentrations are compared in Fig. 5. The average $PM_{1.0}$ and $PM_{2.5}$ levels were highest during winter at 16.3 $\mu g\,m^{-3}$ and 20.3 $\mu g\,m^{-3}$, respectively, followed by spring, when the highest seasonal PM_{10} was observed (35.2 $\mu g\,m^{-3}$). The enhanced mass concentrations were associated with anthropogenic sources, mostly from the Asian continent during the winter monsoon season and with Asian dust events in the spring. The lowest mass concentrations at all sizes were due to frequent rain and small continental effects during the summer season (Lim et al., 2010a, b). While sulfate was most abundant during spring with a fraction of 20–38 %, nitrate was the highest during

ACPD
11, 20521–20573, 2011

winter, with a fraction of 7–11 %. The occurrence of the highest sulfate fraction in spring compared with other seasons was due to the combination of enough SO_2 sources mainly from Asian continent and favorable meteorological conditions for converting SO_2 to sulfate. In summer, on the other hand, sulfate concentrations were low because of the lowest SO_2 concentrations below 1.0 ppbv even under favorable conditions for sulfate conversion and wet removal of precursor gases and particles. Seasonal nitrate levels were inversely related to ambient temperature, being highest in winter at 7–11 %, moderate in spring and fall at 5–9 %, and lowest in summer at 3–8 %.

In this study, carbonaceous fractions were higher in summer and fall under low mass and sulfate concentrations but lower in winter and spring under high mass and sulfate concentrations. Particularly, the OC and EC fractions of $PM_{1.0}$ were highest in fall. It is likely due to the formation of secondary organic aerosols from biomass burning. In spring, biomass burning also takes place but its effect is diluted by high anthropogenic emissions of sulfur and nitrogen. In addition, most of the fall samples were taken under stable atmospheric conditions, which were favorable for the formation and buildup of secondary organic aerosols and pollutants.

5 Characteristics of EC

The EC was compared with BC measured by Aethalometer (Fig. 6a). In contrast to EC quantification by thermochemical analysis, BC concentration was obtained by optical analysis, which estimates light absorption of particles and converts it into mass concentration. The slope of the regression equation of $PM_{1.0}$ EC against BC at 880 nm was 1.0, whereas the slope for PM_{10} EC against BC was 1.5. This result implies that mass absorption efficiency is higher for smaller particles and that the greater fraction of coarse EC may not absorb as much BC as fine EC does.

It can be seen in Fig. 6b that EC and sulfate were well correlated. Due to condensation processes or cloud processing, atmospheric EC is mixed with scattering aerosols (such as sulfate and organic carbon) and can acquire non-absorbing coatings. Although we cannot estimate its mixing state from our data, EC can be

ACPD
11, 20521–20573, 2011

sufficiently mixed with sulfate in places under the influence of substantial anthropogenic sources. That is why sulfate shows not only a good correlation with scattering efficiency measured by Nephelometer but also a reasonable correlation with BC measured by Aethalometer (Table 3). EC was also well correlated with scattering efficiency and BC. It has been shown that more hygroscopic particles, such as sulfate of a given size, will grow more under humid conditions, scattering more incident light (Jimenez et al., 2009). Other studies have reported Mie calculations of soot particles with sulfate coatings showing enhanced absorption (Martins et al., 1998; Fuller et al., 1999). These results suggest a positive contribution of sulfate coatings to net warming.

EC is not a single chemical compound. It can be subdivided into two classes based on our analytical method: char-EC and soot-EC. Char was defined as carbonaceous material obtained by heating organics and formed directly from pyrolysis or as an impure form of graphitic carbon obtained as a residue when carbonaceous material is partially burned or heated with a limited supply of air. Soot was defined as only those carbon particles that form at high temperature via gas-phase processes. Previous studies showed that char and soot had different chemical and physical properties (Kuhlbusch, 1997; Masiello, 2004), as well as optical properties (Bond, 2001; Bond et al., 2002; Kirchstetter et al., 2004). We adopted the operational definitions of EC fractions that Han et al. (2010) suggested to demonstrate the different characteristics of char and soot, based on their previous lab experiment (Han et al., 2007). Their experiment result supported the use of the TOR method to discriminate between char- and soot-EC. The activation energy was lower for char- than soot-EC; char materials always oxidized at low-temperature (550°, at EC1 stage), while Diesel and n-hexane soot samples exhibited similar EC2 peaks (at 700°) and carbon black samples peaked at both EC2 and EC3 (800°). In our study, therefore, char-EC and soot-EC are operationally defined as EC1 and as EC2+3, respectively. In the present work, the mean EC1 concentrations were almost two times higher than the mean EC2+3 concentrations for all size cuts, ranging from 0.96 $\mu g\,m^{-3}$ to 1.39 $\mu g\,m^{-3}$ for EC1 and from 0.30 $\mu g\,m^{-3}$ to 0.46 $\mu g\,m^{-3}$ for EC2+3.

ACPD
11, 20521–20573, 2011

We compared the relationships between EC1 and EC2+3 in the different seasons. They showed the strongest correlation in winter and spring ($R^2 = 0.4 - 0.6$ for $PM_{1.0}$, $PM_{2.5}$, and PM_{10}), which suggests common combustion sources such as biomass burning, residential heating, and coal combustion. In contrast, they were poorly correlated in summer ($R^2 = 0.03 - 0.2$ for $PM_{1.0}$, $PM_{2.5}$, and PM_{10}), which was likely due to reduced burning sources. Furthermore, the overall correlation between EC1 and EC2+3 was better in PM_{10} rather than $PM_{1.0}$. This seems to be associated with particle size: EC1 has larger size (~1–100 μm) than EC2+3, which is emitted as gas or smaller particles (~hundreds of nm).

Although, generally, the concentration of aerosols in the study area is mainly determined by the amounts of emission from the Asian continent, transport processes and wet scavenging as well as emission have an effect on the level of each material. Here, we examined the impact of precipitation on the mass difference between EC1 and EC2+3 using the ratio of the concentration during non-rainy days (31 days) to the concentration during rainy days (10 days) (Table 4). EC2+3 showed little wet scavenging effect with a ratio of 1.0 ~ 1.3. On the other hand, EC1 had a difference in concentration between non-rainy and rainy days. These results imply a longer residence time of EC2+3 in the atmosphere, meaning that soot aerosols are suspended and transported longer. In general, since char-EC is composed of large particles (>~1 μm) as well as small particles, it could be easily removed by wet deposition. Soot, consisting of submicron particles of grape-like clusters, can remain suspended for time scales of the order of a month (Ogren and Charlson, 1983) and has strong light absorption characteristics with little spectral dependence (Schnaiter et al., 2003; Kirchstetter et al., 2004). Thus soot could have greater consequence for warming.

The soot-EC/char-EC ratio depends upon the mixing function of the different sources: motor vehicle emissions and possibly grass burning result in higher soot-EC/char-EC ratios, while wood combustion, particularly biomass burning by smoldering at low temperature, produces lower soot-EC/char-EC ratios (Chow et al., 2004; Chen et al., 2007). In coal combustion, this ratio can be very low or relatively high,

ACPD
11, 20521–20573, 2011

depending on the type of coal (Han et al., 2010). To apply the definitions of Han et al. (2010) to our study, we compared seasonal EC2+3/EC1 ratios (Fig. 7). Seasonally averaged EC1 concentration was highest in winter and lowest in summer. This order is very well matched with the intensity of continental outflows. In contrast, EC2+3 did not show clear seasonal variation, but the highest concentrations were found in spring and the lowest concentrations in fall and winter. As a result, the ratios of EC2+3/EC1 were highest in summer, when all air masses reached at Gosan from the east passing through South Korea or/and Japan with the least influence by the continent and greater influence by South Korea and Japan (See Fig. 9e). EC2+3 emitted during winter and spring may have remained suspended in the atmosphere due to its smaller size and kept its proportion through increased motor vehicle sources from South Korea and Japan, in spite of the wet scavenging caused by frequent precipitation during summer. Han et al. (2010) collected EC particles in Xi'an, a sandland in China, of which result are consistent with our observation that EC1 had a minimum level in summer, but in contrast to our observations, the level of EC2+3 was also minimum in summer. Higher EC2+3 concentrations during summer in our data imply increased influence of South Korea and Japan on EC concentrations. Hence, EC2+3 is considerably enhanced, but EC1 is markedly less because of limited contact with industrial regions in China. Therefore, our study supports the classification of char-EC and soot-EC proposed by Han et al. (2010), and the ratio of EC2+3 to EC1 can serve as an indication of a continental effect. This result agrees well with air mass trajectories, which will be discussed in the following section. For example, the EC2+3/EC1 ratios for the days shown in Fig. 9 are (a) 0.96, (b) 0.17, (c) 0.32, (d) 0.47, and (e) 1.79.

Except for summer, EC1 was closely correlated with potassium, which, among the water-soluble ions, is traditionally well known as an indication of biomass burning (Silva et al., 1999; Guazzotti et al., 2003). Because char-EC has a wide variety of sources and its concentration itself does not provide accurate information about the source, this approach can suggest the contribution of biomass burning to EC1 concentration in different seasons. For the whole measurements, non-sea-salt potassium (nss-K^+)

ACPD
11, 20521–20573, 2011

accounted for ~50–99 %, which could be associated with mineral dust as well as combustion aerosols. In PM_{10}, nss-K^+ was well correlated with nss-SO_4^{2-} ($R^2 = 0.70$), but moderately correlated with nss-Ca^{2+} ($R^2 = 0.53$). In addition, nss-K^+ and nss-SO_4^{2-} showed similarity in size distribution of being enriched in fine mode. Among OC subcomponents, OC2, thought to be secondary, was significantly correlated with sulfate and potassium. In the airborne measurements of trace elements produced from savanna biomass burning, Gaudichet et al. (1995) indicated that near the emission, K was mainly present as KCl, evolving to K_2SO_4 in the ambient samples. Thus, our potassium would be likely to represent the effect of biomass burning, even if it may include some of fossil fuel combustion, dust, and sea salt as well.

Li et al. (2006) quantified EC and OC concentrations in Horquin sandland in northeastern China by a thermal method and reported the strongest correlation of EC with potassium among five elements, suggesting a significant contribution of rural biomass burning to regional carbonaceous aerosol concentrations. A previous study estimated the emissions of BC in China and pointed out that biomass burning is one of the main sources of BC in China (Streets et al., 2003). Gustafsson et al. (2009) used ^{14}C to distinguish fossil fuel and biomass-burning contributions to BC during pollution events in South Asia. They found a far larger contribution of biomass combustion to BC emissions. Biomass burning occurs on a global scale by fires due to slash-and-burn land clearance, waste burning in agriculture and forestry, and residential wood combustion. In particular, East Asia contains biomass burning sources in undeveloped regions of China, Siberia, and North Korea. Biomass combustion-derived materials are likely generated throughout, with the strongest correlations in winter and spring, and transported to the study area. In summer, it is possible that reduced burning and relatively increased sea-salt potassium (ss-K^+) lead to a poor correlation between EC1 and potassium, and that EC1 may deposit on the surface of larger and hygroscopic ss-K^+, leading to better correlation in PM_{10} than $PM_{1.0}$. It is less likely that Siberian wildfires or biomass burning in eastern China had influence on EC1 level of summer samples (Kim et al., 2007).

ACPD
11, 20521–20573, 2011

6 Source fingerprint

To examine the source signature of aerosols and the effect of transport paths on aerosol composition, we categorized air masses into 5 regimes based on meteorological and chemical characteristics and air mass trajectories every 3 h using the FLEXPART Lagrangian particle dispersion model (Stohl et al., 2005) (Fig. 9). In this analysis, samples which were affected by precipitation or did not show constant trajectories in time were excluded. The five types are labeled "Siberia", "Beijing", "Shanghai", "Yellow Sea", and "East Sea" according to the major geographical regions over which an air mass passed during transport. The Siberia, Beijing, Shanghai, Yellow Sea, and East Sea types included 6 days from October to March, 10 days from October to May, 4 days from October to May, 2 days in April, and 6 days from June to September, respectively. The characteristic regimes of each air type are summarized in Table 5. It should be noted that the study region is heavily affected by the monsoon system, and stagnant conditions often developed during transition periods, when trajectories tended to spread over wider areas.

From late fall to early spring, the study region is under the influence of frontal system in association with a Siberian high that is periodically extends towards the southeastern China. As a high pressure approaches, air is usually transported directly from Siberia to Jeju along with a trough. Then high pressure center shifts its way to the southeast and wind turns to northwesterly. While the former represents the continental background air descending from the free troposphere in Siberian region, the latter is classified as Beijing type air that passed fast over Mongolia and Beijing region. As the high pressure is weakened, the air slowly moves down to the southern part of China or over the Yellow Sea before reaching Gosan. The former is classified as Shanghai type that captured the emissions from the southern (Shanghai) as well as northern (Beijing) part of China. The latter is Yellow Sea that is mainly influenced by the Bohai Bay area and in part the west coast of the Korean peninsula. The air mass labeled East Sea was influenced by the East Sea, including Japan and South Korea, and was the most frequently observed

ACPD
11, 20521–20573, 2011

air mass in summer. Siberia type can be regarded as clean background air of the northeast Asia (Fig. 9a). The Beijing and Shanghai types represent fresh continental and aged continental plume, respectively (Fig. 9b and c). As being aged over the ocean, the Yellow Sea type exhibits characteristics of continental plumes (Fig. 9d) and is distinguished from East Sea type air (Fig. 9e).

For each air mass category, the ratios of major constituents in submicron and supermicron aerosols are compared in Table 6. Siberia air showed the lowest levels of CO, sulfate, and $PM_{1.0}$ mass concentrations, resulting in high ratios of chemical constituents. In Beijing type air, the ratios of OP, EC1, and nitrate to mass were the highest. In contrast, an enhanced sulfate/mass ratio was recognizable in Shanghai and Yellow Sea air masses. For these two air masses, the high sulfate content was the result of favorable meteorological conditions such as weak winds and high relative humidity over a warm sea surface (Fig. 9c and d) (Lim et al., 2010a, b) in conjunction with sources from nearby land. The higher nitrate/sulfate ratios in Beijing type air mass are largely due to the temperature dependency of nitrate because the Beijing air was more frequently encountered at Gosan in the colder seasons. Therefore, Beijing and Shanghai plumes were unambiguously differentiated by the ratios of EC1, OP, and nitrate against sulfate.

It is noteworthy that the OC2 fraction against total carbon was also much higher in the Yellow Sea and East Sea types, which could be characterized as relatively aged marine air masses (Fig. 9d and e). It is supporting evidence for the secondary nature of OC2, such that its ratio to TC tended to be higher in the smaller particle sizes (Fig. 3j). In addition, the ratio of EC2+3 to EC1 was distinctly higher in the East Sea air mass. This result agrees with the findings of Han et al. (2010) and this study that the ratio of EC2+3 to EC1 can serve as an indicator of continental effects and suggests a greater influence of motor vehicle emissions from South Korea and Japan, with a reduced influence from China. This ratio is also likely to be increased in aged air due to the longer lifetime of EC2+3 than EC1, as discussed in the previous section.

ACPD
11, 20521–20573, 2011

In the present study, OP was recognized as a major component of OC and found to be a source signature of the Beijing type air mass. Through the entire period of observation, OP was noticeably elevated when wind speed was high under the influence of a strong continental high or a migratory cyclone. As a result, high ratios of OP to EC1 were observed in fast-moving air parcels carried by northwesterly winds in winter or northerly winds in spring, which could bring relatively fresh emissions from Beijing and its vicinity and plumes due to biomass burning in Mongolia (Kim et al., 2007) and Siberia if they existed (Fig. 9a). In contrast, OP remained low in the warmer seasons, which were characterized by stagnant air masses, leading to low OP/EC ratios. These variations are evident in Table 6, in which it can be seen that the ratio of OP/EC1 was quite low in Yellow Sea and East Sea air masses. Therefore, the main sources of OP are likely to be coal combustion and biomass burning.

OP is defined as charred OC having characteristics similar to those of EC1; that is, it is likely a light-absorbing aerosol. The BC absorption spectrum measured by Aethalometer revealed different tendencies among 7 wavelengths (Lim et al., 2011), for some of which the absorption of short wavelength (370 nm) was greater than that of longer wavelengths. It is generally known that soot, which is composed of submicron particles of grape-like clusters, exhibits strong light absorption characteristics with little spectral dependence (Schnaiter et al., 2003; Kirchstetter et al., 2004). In the present study, the enhanced absorption of shortwave radiation was clear for samples containing large amounts of OP. Thus, we believe that OP is light-absorbing organic carbon or a strong candidate for brown carbon. It has been reported in previous studies that particles from smoldering combustion (Patterson and McMahon, 1984), residential coal combustion (Bond, 2001), or biogenic emissions of humics and lignin (Andreae and Gelencsér, 2006) can contain substantial amounts of brown carbon. Clarke et al (2007) found enhanced shortwave absorption by refractory OC from biomass burning, which was likely to be a primary aerosol.

Although EC and BC have long been major topics of research due to their light-absorbing characteristics, the recent discovery of light-absorbing carbon, called brown

ACPD
11, 20521–20573, 2011

carbon, makes it imperative to reassess and redefine the components that make up light-absorbing carbonaceous matter in the atmosphere (Andreae and Gelencsér, 2006; Alexander et al., 2008). There is a continuum of carbonaceous substances in atmospheric aerosols, where refractory organics included in a thermochemical classification are consistent with colored organics in an optical classification. These so-called brown carbons have a sharply increased absorption efficiency toward shorter wavelengths, although the absorption is much less than that of soot carbon at the wavelength of 550 nm, and this spectral dependence causes the material to appear brown and makes their absorption in the UV potentially significant due to the large amounts occurring in continental aerosols (Kirchstetter et al., 2004; Hoffer et al., 2006). However, their optical properties, origin, and chemical composition are poorly understood and thus need further investigation.

The results discussed above highlight the fact that the Beijing air mass is distinguished not only by higher ratios of EC1 and OP to mass but also by higher ratios of EC1 (and OP) to sulfate. This implies that air masses from the Beijing area may have a more significant influence on net warming than do air masses from the other regions. This result confirms the main conclusion of Ramana et al. (2010), who estimated the impact of BC/sulfate ratios of air masses transported from the Beijing and Shanghai areas on net warming based on surface and aircraft measurements conducted over the Yellow Sea in spring and summer.

7 Conclusions

Daily $PM_{1.0}$, $PM_{2.5}$, and PM_{10} samples were taken at Gosan ABC Superstation on Jeju Island from August 2007 to September 2008. The mass concentrations of $PM_{1.0}$, $PM_{2.5}$, and PM_{10} varied between 1.26 $\mu g\,m^{-3}$ and 29.51 $\mu g\,m^{-3}$, 3.94 $\mu g\,m^{-3}$ and 39.17 $\mu g\,m^{-3}$, and, 7.52 $\mu g\,m^{-3}$ and 69.76 $\mu g\,m^{-3}$, respectively. $PM_{1.0}$ and $PM_{2.5}$ account for 48.4 % and 79.6 % of PM_{10}, respectively, indicating a large portion of fine-mode aerosols in this study area. EC tended to be enriched in smaller particles and

ACPD
11, 20521–20573, 2011

made up 10.4 %, 9.8 %, and 6.0 % of $PM_{1.0}$, $PM_{2.5}$, and PM_{10}, respectively. Unlike EC, OC accounted for 23.0 %, 22.9 %, and 16.4 % in $PM_{1.0}$, $PM_{2.5}$, and PM_{10}, respectively. The size distributions of OC subcomponents such as OC3 and OC4 reflected substantial contributions of primary sources such as dust, sea salt, or biogenic matter.

The definition and measurement techniques for atmospheric EC (or BC) have long been subjects of scientific controversy. We compared our observed EC with BC measurements obtained by Aethalometer and found a perfect relationship with a slope of 1.0 for $PM_{1.0}$ EC1 (but not for PM_{10}). This result indicates that coarse particles have lower light-absorbing efficiency than fine particles. In our data, EC and sulfate were well correlated, meaning that there is difficulty in distinguishing absorbing aerosols from scattering aerosols. For EC, the definition of EC1 as char-EC and EC2+3 as soot-EC applied well to our measurements; the former is emitted from smoldering combustion (such as biomass burning and residential and coal combustion), and the latter is generated from flaming combustion (such as motor vehicle exhaust and coal combustion). The mean EC1 concentrations were almost two times higher than the mean EC2+3 concentrations for all three particle sizes, ranging from 0.96 $\mu g\,m^{-3}$ to 1.39 $\mu g\,m^{-3}$ for EC1 and from 0.30 $\mu g\,m^{-3}$ to 0.46 $\mu g\,m^{-3}$ for EC2+3. EC1 was strongly correlated with potassium throughout the year except for summer. While EC2+3 was more enriched in $PM_{1.0}$, EC1 favored $PM_{2.5}$ or PM_{10}. As a result, EC1 was more sensitive to wet scavenging, and the ratio of EC1 to EC2+3 was higher in summer. This difference was likely linked with a longer residence time of EC2+3 than that of EC1 in the atmosphere. This result implies a role of EC2+3 as a contribution to warming, particularly at a regional scale, due to its longer lifetime, even though its concentrations in the atmosphere are lower.

This study highlights the ratios of major chemical species as useful tools to distinguish the main sources of aerosols and the degree of atmospheric processing. Five air mass types were clearly identified: Siberia, Beijing, Shanghai, Yellow Sea, and East Sea types. Siberian types would be regarded as continental background air of the northeast Asia. While the Beijing, Shanghai, and Yellow Sea air masses were mostly

ACPD
11, 20521–20573, 2011

influenced by China, the Korean emissions affected the Yellow Sea and East Sea type air masses. For the East Sea air, Japanese and Korean influences were dominant. The Beijing type air was the freshest and was distinguished by higher concentrations of EC and OP relative to sulfate, signifying a higher net warming effect of aerosols in this air type than in the other three types. OP was also suggested as a light-absorbing form of carbon. On the other hand, sulfate was remarkably enhanced in air that had been slowly transported over China or the Yellow Sea, which was the case of the Shanghai and Yellow Sea air masses. The aged air masses of Yellow Sea and East Sea types in particular showed lower OP to sulfate ratios and higher OC2 to TC ratios. The latter implies a secondary role among OC fractions in conjunction with a tendency of enrichment at smaller aerosol sizes. Furthermore, the highest ratio of EC2+3 to EC1 was found in the East Sea air, in sharp contrast with the other air mass categories, which showed more impact of Chinese emissions.

Acknowledgements. Authors thank to Stohl for allowing us to use Flexpart results at Gosan. This study was supported by the Korea Research Foundation through a grant KRF-2008-314-C00402.

References

Aggarwal, S. G. and Kawamura, K.: Carbonaceous and inorganic composition in long-range transported aerosols over northern Japan: Implication for aging of water-soluble organic fraction, Atmos. Environ., 43,(16), 2532–2540, 2009.

Akimoto, Hajime: Global Air Quality and Pollution, Science, 302, 5651, 1716–1719, doi:10.1126/science.1092666, 2003.

Alexander, D. T. L., Crozier, P. A., and Anderson, J. R.: Brown Carbon Spheres in East Asian Outflow and Their Optical Properties, Sci., 321, 833–836, doi:10.1126/science.1155296, 2008.

Andreae, M. O. and Gelencsér, A.: Black carbon or brown carbon? The nature of light-absorbing carbonaceous aerosols, Atmos. Chem. Phys., 6, 3131–3148, doi:10.5194/acp-6-3131-2006, 2006.

ACPD

11, 20521–20573, 2011

Andrews, E., Saxena, P., Musarra, S., Hildemann, L. M., Koutrakis, P., McMurry, P. H., Olmez, I., and White, W. H.: Concentration and composition of atmospheric aerosols from the 1995 SEAVS experiment and a review of the closure between chemical and gravimetric measurements, J. Air Waste Manage. Assoc., 50, 648–664, 2000.

Bassett, M. E. and Seinfeld, J. H.: Atmospheric equilibrium model of sulfate and nitrate aerosols-II. Particle size analysis, Atmos. Environ., 18, 1163–1170, 1984.

Bond, T. C.: Spectral dependence of visible light absorption by carbonaceous particles emitted from coal combustion, Geophys. Res. Lett., 28, 4075–4078, doi:10.1029/2001GL013652, 2001.

Bond, T. C., Covert, D. S., Kramlich, J. C., Larson, T. V., and Charlson, R. J.: Primary particle emissions from residential coal burning: Optical properties and size distributions, J. Geophys. Res., 107(D21), 8347, doi:10.1029/2001JD000571, 2002.

Bond, T. C., Habib, G., and Bergstrom, R. W.: Limitations in the enhancement of visible light absorption due to mixing state, J. Geophys. Res., 111, D20211, doi:10.1029/2006JD007315, 2006.

Bond, T. C., Bhardwaj, E., Dong, R., Jogani, R., Jung, S., Roden, C., Streets, D. G., and Trautmann, N. M.: Historical emissions of black and organic carbon aerosols from energy-related combustion, 1850–2000, Global Biogeochem. Cy., 21, GB2018, doi:10.1029/2006GB002840, 2007.

Brasseur, G. P., Orlando, J. J., and Tyndall, G. S.: Atmospheric Chemistry and Global Change. Oxford University Press., Oxford, UK, 654, 1999.

Buzorius, G., McNaughton, C. S., Clarke, A. D., Covert, D. S., Blomquist, B., Nielsen, K., and Brechtel, F. J.: Secondary aerosol formation in continental outflow conditions during ACE-Asia, J. Geophys. Res., 109(15), D24203, doi:10.1029/2004JD004749, 2004.

Cao, J. J., Lee, S. C., Ho, K. F., Zhang, X. Y., Zou, S. C., Fung, K., Chow, J. C., and Watson, J. G.: Characteristics of carbonaceous aerosol in Pearl River Delta Region, China during 2001 winter period, Atmos. Environ., 37, 11, 1451–1460, 2003.

Cao, J. J., Wu, F., Chow, J. C., Lee, S. C., Li, Y., Chen, S. W., An, Z. S., Fung, K. K., Watson, J. G., Zhu, C. S., and Liu, S. X.: Characterization and source apportionment of atmospheric organic and elemental carbon during fall and winter of 2003 in Xi'an, China, Atmos. Chem. Phys., 5, 3127–3137, doi:10.5194/acp-5-3127-2005, 2005.

Carmichael, G. R., Zhang, Y., Chen, L. L., Hong, M. S., and Ueda, H. : Seasonal variation of aerosol composition at Cheju Island, Korea, Atmos. Environ., 30, 2407–2416, 1996.

ACPD

11, 20521–20573, 2011

Carmichael, G. R., Hong, M. S., Ueda, H., Chen, L. L., Murano, K., Park, J. K., Lee, H. G., Kim, Y., Kang, C., and Shim, S.: Aerosol composition at Cheju Island, Korea, J. Geophys. Res., 102, 6047–6061, doi:10.1016/1352-2310(95)00230-8, 1997.

Chen, L.-L., Carmichael, G. R., Hong, M., Ueda, H., Shim, S., Song, C. H., Kim, Y. P., Arimoto, R., Prospero, J., Savoie, D., Murano, K., Park, J. K., Lee, H., and Kang, C.: Influence of continental outflow events on the aerosol composition at Cheju Island, South Korea, J. Geophys. Res., 102(D23), 28551–28574, doi:10.1029/97JD01431, 1997.

Chen, L.-W. A., Moosmuller, H., Arnott, W. P., Chow, J. C., Watson, J. G., Susott, R. A., Babbitt, R. E., Wold, C. E., Lincoln, E. N., and Hao, W. M.: Emissions from laboratory combustion of wildland fuels: Emission factors and source profiles, Environ. Sci. Technol., 41, 4317–4325, 2007.

Chow, J. C., Watson, J. G., Kuhns, H. D., Etyemezian, V., Lowenthal, D. H., Crow, D. J., Kohl, S. D., Engelbrecht, J. P., and Green, M.C.: Source profiles for industrial, mobile, and area sources in the Big Bend Regional Aerosol Visibility and Observational (BRAVO) Study, Chemos., 54, 185–208, doi:10.1016/j.chemosphere.2003.07.004, 2004.

Chow, J. C., Watson, J. G., Louie, P. K., Chen, L. W., and Sin, D.: Comparison of PM2.5 carbon measurement methods in Hong Kong, China, Environ. Pollut., 137(2), 334–344, 2005.

Clarke, A., McNaughton, C., Kapustin, V., Shinozuka, Y., Howell, S., Dibb, J., Zhou, J., Anderson, B., Brekhovskikh, V., Turner, H., and Pinkerton, M.: Biomass burning and pollution aerosol over North America: Organic components and their influence on spectral optical properties and humidification response, J. Geophys. Res., 112, D12S18, doi:10.1029/2006JD007777, 2007.

Decesari, S., Facchini, M. C., Matta, E., Mircea, M., Fuzzi, S., Chughtai, A. R., and Smith, D. M.: Water soluble organic compounds formed by oxidation of soot, Atmos. Environ., 36(30), 1827–1832, 2002.

Dentener, F. J., Carmichael, G. R., Zhang, Y., Lelieveld, J., and Crutzen, P. J.: Role of mineral aerosol as a reactive surface in the global troposphere. J. Geophys. Res., 101, 22869–22889, doi:10.1029/96JD01818, 1996.

Fuller, K. A., Malm,W. C., and Kreidenweis, S. M.: Effects of mixing on extinction by carbonaceous particles, J. Geophys. Res., 104, 15941–15954, 1999.

Gaudichet, A., Echalar, F., Chatenet, B., Quisefit, J. P., Malingre, G., Cachier, H., Artaxo, P., Maenhaut, W., and Buat-M'enard, P.: Trace elements in tropical African savannah biomass burning aerosol, J. Atmos. Chem., 22, 19–39, 1995.

ACPD
11, 20521–20573, 2011

Geng, H., Park, Y., Hwang, H., Kang, S., and Ro, C.-U.: Elevated nitrogen-containing particles observed in Asian dust aerosol samples collected at the marine boundary layer of the Bohai Sea and the Yellow Sea, Atmos. Chem. Phys., 9, 6933–6947, doi:10.5194/acp-9-6933-2009, 2009.

Gray, H. A., Cass, G. R., Huntzicker, J. J., Heyerdahl, E. K., and Rau, J. A.: Characteristics of atmospheric organic and elemental carbon particle concentrations in Los Angeles, Environ. Sci. Technol., 20, 580–582, doi:10.1021/es00148a006, 1986.

Guazzotti, S. A., Suess, D. T., Coffee, K. R., Quinn, P. K., Bates, T. S., Wisthaler, A., Hansel. A., Ball, W. P., Dickerson, R. R., Neusüß, C., Crutzen, P. J., Prather, K. A.: Characterization of carbonaceous aerosols outflow from India and Arabia: Biomass/biofuel burning and fossil fuel combustion, J. Geophys. Res., 108, D15, doi:10.1029/2002JD003277, 2003.

Gustafsson, Ö., Kruså, M., Zencak, Z., Sheesley, R. J., Granat, L., Engström, E., Praveen, P. S., Rao, P. S. P., Leck, C., and Rodhe, H.: Brown clouds over South Asia: Biomass or fossil fuel combustion?, Science, 323(5913), 495–498, doi:10.1126/science.1164857, 2009.

Hagler, G. S. W., Bergin, M. H., Salmon, L. G., Yu, J. Z., Wan, E. C. H., Zheng, M., Zeng, L. M., Kiang, C. S., Zhang, Y. H., Lau, A. K. H., and Schauer, J. J.: Source areas and chemical composition of fine particulate matter in the Pearl River Delta region of China, Atmos. Environ., 40(20), 3802–3815, 2006.

Han, Y. M., Cao, J., Chow, J. C., Watson, J. G., An, Z., Jin, Z., Fung, K., and Liu, S.: Evaluation of the thermal/optical reflectance method for discrimination between char- and soot-EC, Chemosphere, 69, 569–574, doi:10.1016/j.chemosphere.2007.03.024, 2007.

Han, Y. M., Cao, J.J., Lee, S. C., Ho, K. F., and An, Z. S.: Different characteristics of char and soot in the atmosphere and their ratio as an indicator for source identification in Xi'an, China, Atmos. Chem. Phys., 10, 595–607, doi:10.5194/acp-10-595-2010, 2010.

Hansen, J., Sato, M., and Ruedy, R.: Radiative forcing and climate response. J. Geophys. Res., 102(D6), 6831–6864, doi:10.1029/96JD03436, 1997.

Havers, N., Burba, P., Lambert, J., and Klockow, D.: Spectroscopic characterization of humic-like substances in airborne particulate matter, J. Atmos. Chem., 29, 45–54, doi:10.1023/A:1005875225800, 1998.

Haywood, J. and Boucher, O.: Estimates of the direct and indirect radiative fording due to tropospheric aerosols: A review, Rev. Geophys., 38(4), 513–543, doi:10.1029/1999RG000078, 2000.

Hoffer, A., Gelencsér, A., Guyon, P., Kiss, G., Schmid, O., Frank, G. P., Artaxo, P., and Andreae,

ACPD

11, 20521–20573, 2011

M. O.: Optical properties of humic-like substances (HULIS) in biomass-burning aerosols, Atmos. Chem. Phys., 6, 3563–3570, doi:10.5194/acp-6-3563-2006, 2006.
Huebert, B. J., Bates, T., Russell, P. B., Shi, G., Kim, Y. J., Kawamura, K., Carmichael, G., and Nakajima, T.: An overview of ACE-Asia: Strategies for quantifying the relationships between Asian aerosols and their climatic impacts, J. Geophys. Res., 108(D23), 8633, doi:10.1029/2003JD003550, 2003.
IPCC: (2007) in: Climate Change 2007: The Physical Science Basis (Contribution of Working Group I to the Fourth Assessment Report of the Intergovernmental Panel on Climate Change) edited by: Solomon, S., Qin, D. Manning, M., Chen, Z., Marquis, M., Averyt, K. B., Tignor, M., and Miller, H. L., Cambridge Univ. Press, New York, 131–217, 2007.
Jacobson, M. C., Hansson, H.-C., Noone, K. J., and Charlson, R. J.: Organic atmospheric aerosols: review and state of the science, Rev. Geophys., 38, 267–294, doi:10.1029/1998RG000045, 2000.
Jacobson, M. Z.: Strong radiative heating due to the mixing state of black carbon in atmospheric aerosols, Nature, 409, 695–697, doi:10.1038/35055518, 2001.
Jimenez, J. L., Canagaratna, M. R., Donahue, N. M., Prevot, A. S. H., Zhang, Q., Kroll, J. H., DeCarlo, P. F., Allan, J. D., Coe, H., Ng, N. L., Aiken, A. C., Docherty, K. S., Ulbrich, I. M., Grieshop, A. P., Robinson, A. L., Duplissy, J., Smith, J. D., Wilson, K. R., Lanz, V. A., Hueglin, C., Sun, Y. L., Tian, J., Laaksonen, A., Raatikainen, T., Rautiainen, J., Vaattovaara, P., Ehn, M., Kulmala, M., Tomlinson, J. M., Collins, D. R., Cubison, M. J., E., Dunlea, J., Huffman, J. A., Onasch, T. B., Alfarra, M. R., Williams, P. I., Bower, K., Kondo, Y., Schneider, J., Drewnick, F., Borrmann, S., Weimer, S., Demerjian, K., Salcedo, D., Cottrell, L., Griffin, R., Takami, A., Miyoshi, T., Hatakeyama, S., Shimono, A., Sun, J. Y., Zhang, Y. M., Dzepina, K., Kimmel, J. R., Sueper, D., Jayne, J. T., Herndon, S. C., Trimborn, A. M., Williams, L. R., Wood, E. C., Middlebrook, A. M., Kolb, C. E., Baltensperger, U., and Worsnop, D. R.: Evolution of Organic Aerosols in the Atmosphere, Science, 326(5959), 1525, doi:10.1126/science.1180353, 2009.
Kanakidou, M., Seinfeld, J. H., Pandis, S. N., Barnes, I., Dentener, F. J., Facchini, M. C., Van Dingenen, R., Ervens, B., Nenes, A., Nielsen, C. J., Swietlicki, E., Putaud, J. P., Balkanski, Y., Fuzzi, S., Horth, J., Moortgat, G. K., Winterhalter, R., Myhre, C. E. L., Tsigaridis, K., Vignati, E., Stephanou, E. G., and Wilson, J.: Organic aerosol and global climate modelling: a review, Atmos. Chem. Phys., 5, 1053–1123, doi:10.5194/acp-5-1053-2005, 2005.
Kim, Y. P., Moon, K.-C., and Lee, J. H.: Organic and elemental carbon in fine particles at Kosan,

ACPD
11, 20521–20573, 2011

Korea, Atmos. Environ., 34(20), 3309–3317, 2000.
Kim, S.-W., Yoon, S.-C., Kim, J., and Kim, S.-Y.: Seasonal and monthly variations of columnar aerosol optical properties over east Asia determined from multi-year MODIS, LIDAR, and AERONET Sun/sky radiometer measurements, Atmos. Environ., 41(8), 1634–1651, doi:10.1016/j.atmosenv.2006.10.044, 2007.
Kirchstetter, T. W., Novakow, T., and Hobbs, P.V.: Evidence that the spectral dependence of light absorption by aerosols is affected by organic carbon, J. Geophys. Res., 109, D21208, doi:10.1029/2004JD004999, 2004.
Koçak, M., Mihalopoulos, N., and Kubilay, N.: Chemical composition of the fine and coarse fraction of aerosols in the Northeastern Mediterranean, Atmos. Environ., 41, 7351–7368, 2007.
Kuhlbusch, T. A. J. and Crutzen, P. J.: Toward a global estimate of black carbon in residues of vegetation fires representing a sink of atmospheric CO_2 and a source of O_2, Global Biogeochem. Cy., 9, 491–501, doi:10.1029/95GB02742, 1995.
Kuhlbusch, T. A. J.: Black carbon in soils, sediments, and ice cores, in: Environmental analysis and remediation, edited by: Meyers, R. A., John Wiley & Sons, Toronto, Canada, 813–823, 1997.
Lee, M., Song, M., Moon, K. J., Han, J. S., Lee, G., and Kim, K.-R.: Origins and chemical characteristics of fine aerosols during the northeastern Asia regional experiment (Atmospheric Brown Cloud-East Asia Regional Experiment 2005), J. Geophys. Res., 112, D22S29, doi:10.1029/2006JD008210, 2007.
Lee, J. Y., Kim, Y. P., Bae, G. N., Park, S. M., and Jin, H. C. : The characteristics of particulate PAHs concentrations at a roadside in Seoul, Korean J. Atmos. Environ., 24(2), 133–142, 2008.
Lee, H. W., Lee, T. J., and Kim, D. S.: Identifying Ambient $PM_{2.5}$ Sources and estimating their contributions by using PMF: Separation of gasoline and diesel automobile sources by analyzing ECs and OCs, J. Korean Soc. Atmos. Environ., 25(1), 75–89, 2009.
Li, X., Shen, Z., Cao, J., Liu, S., Zuh, C., and Zhang, T.: Distribution of carbonaceous aerosol during spring 2005 over the Horquin sandland in northeastern China, China Particuology, 4(6), 316–322, doi:10.1016/S1672-2515(07)60282-6, 2006.
Lin, C.-Y., Wang, Z., Chen, W.-N., Chang, S.-Y., Chou, C. C. K., Sugimoto, N., and Zhao, X.: Long-range transport of Asian dust and air pollutants to Taiwan: observed evidence and model simulation, Atmos. Chem. Phys., 8, 2717–2728, 2008,

ACPD
11, 20521–20573, 2011

Lim, S.: Source Signature of Ions and Carbonaceous Compounds in Submicron and Supermicron Aerosols at Gosan-super site, Jeju, South Korea, Master's thesis, Korea University, 2009.

Lim, S., Lee, M., Lee, G., and Kang, K.: Source signature of mass, nitrate and sulfate in supermicron and submicron aerosols at Gosan Superstation on Jeju Island, Atmos., 20(3), 221–228. 2010a.

Lim, S., Lee, M., and Kang, K.: Seasonal Variations of OC and EC in PM_{10}, $PM_{2.5}$ and $PM_{1.0}$ at Gosan Superstation on Jeju Island, Korean J. Atmos. Environ., 26(5), 567–580, 2010b.

Lim, S., Lee, M., Kim, S. Yoon, K., and Kang, E.: Carbonaceous and major inorganic compositions of fine and coarse aerosols in relation to scattering and absorption characteristics at Gosan superstation, soon to be submitted, 2011.

Mace, K. A., Kubilay, N., and Duce, R. A.: Organic nitrogen in rain and aerosol in the eastern Mediterranean: an association with atmospheric dust, J. Geophys. Res., 108, 4320–4330, doi:10.1029/2002JD002997, 2003.

Mamane, Y. and Gottlieb, J.: Heterogeneous reactions of minerals with sulfur and nitrogen oxides, J. Aerosol Sci., 20, 303–311, doi:10.1016/0021-8502(89)90006-2, 1989.

Maria, S. F., Russell, L. M., Gilles, M. K., and Myneni, S. C. B.: Organic aerosol growth mechanisms and their climate-forcing implications, Science, 306(5703), 1921–1924, doi:10.1126/science.1103491, 2004.

Martins, J. V., Artaxo, P., Liousse, C., Reid, J. S., Hobbs, P. V., and Kaufman, Y. J.: Effects of black carbon content, particle size, and mixing on light absorption by aerosols from biomass burning in Brazil, J. Geophys. Res., 103, 32041–32050, 1998.

Masiello, C. A.: New directions in black carbon organic geochemistry, Mar. Chem., 92, 201–213, 2004.

Mochida, M., Umemoto, N., Kawamura, K., Lim, H.-J., and Turpin, B. J.: Bimodal size distributions of various organic acids and fatty acids in the marine atmosphere: Influence of anthropogenic aerosols, Asian dusts, and sea spray off the coast of East Asia, J. Geophys. Res., 112, D15209, doi:10.1029/2006JD007773, 2007.

Moon, K. J., Han, J. S., Ghim, Y. S., and Kim, Y. J.: Source apportionment of fine carbonaceous particles by positive matrix factorization at Gosan background site in East Asia, Environ. Int., 34(5), 654–664, 2008.

Mukai, H. and Ambe, Y.: Characterization of a humic acid-like brown substance in airborne particulate matter and tentative identification of its origin, Atmos. Environ., 20, 813–819,

ACPD

11, 20521–20573, 2011

1986.
Nunes, T. V. and Pio, C. A.: Carbonaceous aerosols in industrial and coastal atmosphere, Atmos. Environ., 27(8), 1339–1346, 1993.
Oen, A. M. P., Schaanning, M., Ruus, A., Cornelissen, G., Källqvist, T., and Breedveld, G. D.: Predicting low biota to sediment accumulation factors of PAHs by using infinite-sink and equilibrium extraction methods as well as BC-inclusive modeling, Chemosphere, 64(8), 1412–1420, doi:10.1016/j.chemosphere.2005.12.028, 2006.
Ohta, S., Hori, M., Yamagata, S., and Murao, N.: Chemical characterization of atmospheric fine particles in Sapporo with determination of water content, Atmos. Environ, 32(6), 1021–1025, 1998.
Ogren, J. A. and Charlson, R. J.: Elemental carbon in the atmosphere: cycle and lifetime, TELLUS SERIES B-CHEMICAL AND PHYSICAL METEOROLOGY, 35B(4), 241–254, doi:10.1111/j.1600-0889.1983.tb00027.x,1983.
Park, S. S., Kim, Y. J., and Fung, K.: Characteristics of $PM_{2.5}$ carbonaceous aerosol in the Sihwa industrial area, Korea, Atmos. Environ., 35(4), 657–665, 2001.
Park, R., Kim, M., Jeong, J., Youn, D., and Kim, S.: A contribution of brown carbon aerosol to the aerosol light absorption and its radiative forcing in East Asia, Atmos. Environ., 44(11), 1414–1421, doi:10.1016/j.atmosenv.2010.01.042, 2010.
Patterson, E. M. and McMahon, C. K.: Absorption characteristics of forest fire particulate matter, Atmos. Environ., 18, 2541–2551, 1984.
Persiantseva, N. M., Popovicheva, O. B., and Shonija, N. K.: Wetting and hydration of insoluble soot particles in the upper troposphere, J. Environ. Monit., 6, 939–945, 2004.
Petzold, A., Gysel, M., Vancassel, X., Hitzenberger, R., Puxbaum, H., Vrochticky, S., Weingartner, E., Baltensperger, U., and Mirabel, P.: On the effects of organic matter and sulphur-containing compounds on the CCN activation of combustion particles, Atmos. Chem. Phys., 5, 3187–3203, doi:10.5194/acp-5-3187-2005, 2005.
Pey, J., Pérez, N., Castillo, S., Viana, M., Moreno, T., Pandolfi, M., López-Sebastián, J.M., Alastuey, A., and Qeurol., X.: Geochemistry of regional background aerosols in the Western Mediterranean, Atmos. Res., 94, 3, 422–435, 2009.
Qu, W. J., Zhang, X. Y., Arimoto, R., Wang, Y. Q., Wang, D., Sheng, L. F., and Fu, G.: Aerosol background at two remote CAWNET sites in western China, Sci Total Environ, 407(11), 3518–3529, 2009.
Ramachandran, S., Rengarajan, R., and Sarin, M. M.: Atmospheric carbonaceous aerosols:

ACPD
11, 20521–20573, 2011

issues, radiative forcing and climate impacts, Cur. Sci. Com., 97, 1, 18–20, 2009.
Ramana, M. V., Ramanathan, V., Feng, Y., Yoon, S-C., Kim, S-W., and Carmichael, G. R.: Warming influenced by the ratio of black carbon to sulphate and the black-carbon source, Nature Geosci., 3, 542–545, doi:10.1038/NGEO918, 2010.
Ramanathan, V., Crutzen, P. J., Kiehl, J. T., and Rosenfeld, D.: Atmosphere – Aerosols, climate, and the hydrological cycle, Science, 294, 5549, 2119–2124, doi:10.1126/science.1064034, 2001.
Ramanathan, V. and Carmichael, G.: Global and regional climate changes due to black carbon, Nature Geosci., 1, 221–227, doi:10.1038/ngeo156, 2010.
Ramanathan, V. and Xu, Y.: The Copenhagen Accord for limiting global warming: Criteria, constraints, and available avenues, PNAS, 107(18), 8055–8062, doi:10.1073/pnas.1002293107, 2010.
Ravishankara, A. R.: Heterogeneous and multiphase chemistry in the Troposphere, Science, 276(5315), 1058–1065, doi:1126/science.276.5315.1058, 1997.
Robertson, A., Overpeck, J., Rind, D., Mosley-Thompson, E., Zielinski, G., Lean, J., Koch, D., Penner, J., Tegen, I., and Healy, R.: Hypothesized climate forcing time series for the last 500 years, J. Geophys. Res., 106, 14783–14803, doi:10.1029/2000JD900469, 2001.
Russell, L. M., Maria, S. F., and Myneni, S. C. B.: Mapping organic coatings on atmospheric particles, Geophys. Res. Lett., 29(16), 1779, doi:10.1029/2002GL014874, 2002.
Schnaiter, M., Horvath, H., Mohler, O., Naumann, K.-H., Saatoff, H., and Schock, O. W.: UV-VIS-NIR spectral optical properties of soot and soot-containing aerosols, J. Aerosol Sci., 34, 1421–1444, doi:10.1016/S0021-8502(03)00361-6, 2003.
Shah, J. J., Johnson, R. L., Heyerdahl, E. K., and Huntzicker, J. J.: Carbonaceous aerosol at urban and rural sites in the United States, J. Air Pollut. Control Assoc., 36, 254–257, 1986.
Shen, Z. X., Cao, J. J., Arimoto, R., Zhang, R. J., Jie, D. M., Liu, S. X., and Zhu, C. S.: Chemical composition and source characterization of spring aerosol over Horqin sand land in northeastern China, J. Geophys. Res., 112, D14315, doi:10.1029/2006JD007991, 2007.
Silva, P. J., Liu, D. Y., Noble, C. A., and Prather, K. A.: Size and chemical characterization of individual particles resulting from biomass burning of local southern California species, Environ. Sci. Technol., 33, 3068, doi:10.1021/es980544p, 1999.
Stohl, A., Forster, C., Frank, A., Seibert, P., and Wotawa, G.: Technical note: The Lagrangian particle dispersion model FLEXPART version 6.2, Atmos. Chem. Phys., 5, 2461–2474, doi:10.5194/acp-5-2461-2005, 2005.

ACPD
11, 20521–20573, 2011

Streets, D. G., Bond, T. C., Carmichael, G. R., Fernandes, S. D., Fu, Q., He, D., Klimont, Z., Nelson, S. M., Tsai, N. Y., Wang, M. Q., Woo, J.-H., and Yarber, K. F.: An inventory of gaseous and primary aerosol emissions in Asia in the year 2000, J. Geophys. Res., 108(D21), GTE30-1-GTE30-23, doi:10.1029/2002JD003093, 2003.

Talbot, R. W., Harriss, P. C., Browell, E. V., Gregory, G. L., Sebacher, D. I., and Beck, S. M.: Distribution and geochemistry of aerosols in the tropical north Atlantic troposphere: relationship to Saharan dust, J. Geophys. Res., 91(D4), 5173–5182, doi:10.1029/JD091iD04p05173, 1986.

Tsigaridis, K., Krol, M., Dentener, F. J., Balkanski, Y., Lathière, J., Metzger, S., Hauglustaine, D. A., and Kanakidou, M.: Change in global aerosol composition since preindustrial times, Atmos. Chem. Phys., 6, 5143–5162, doi:10.5194/acp-6-5143-2006, 2006.

Wang, Y., Zhuang, G., Tang, A., Zhang, W., Sun, Y., Wang, Z., and An, Z.: The evolution of chemical components of aerosols at five monitoring sites of China during dust storms, Atmos. Environ., 41, 1091–1106, 2007.

Worsnop, D. R., Morris, J. W., Shi, Q., Davidovits, P., and Kolb, C. E.: A chemical kinetic model for reactive transformations of aerosol particles, Geophys. Res. Lett., 29(20), 57-1-57-4, doi:10.1029/2002GL015542, 2002.

Wu, P. M. and Okada, K.: Nature of coarse nitrate particles in the atmosphere: a single particle approach, Atmos. Environ., 28, 2053–2060, 1994.

Yang, F., He, K., Ye, B., Chen, X., Cha, L., Cadle, S. H., Chan, T., and Mulawa, P. A.: One-year record of organic and elemental carbon in fine particles in downtown Beijing and Shanghai, Atmos. Chem. Phys., 5, 1449–1457, doi:10.5194/acp-5-1449-2005, 2005.

Zhang, Y., Sunwoo, Y., Kotamarthi, V., and Carmichael, G. R.: Photochemical oxidant processes in the presence of dust: an evaluation of the impact of dust on particulate nitrate and ozone formation, J. Applied Meteorology, 33, 7, 813–824, doi:10.1175/1520-0450(1994)033<0813:POPITP>2.0.CO;2, 1994.

ACPD

11, 20521–20573, 2011

Table 1. The number of sample sets of PM_{10}, $PM_{2.5}$, and $PM_{1.0}$ taken from August 2007 to September 2008.

Year	2007				2008								
Month	Aug	Oct	Nov	Dec	Jan	Feb	Mar	Apr	May	Jun	Aug	Sep	total
No.	1	5	4	2	5	3	4	8	4	1	2	2	41

ACPD
11, 20521–20573, 2011

Table 2. Averaged concentrations of mass and major compositions of $PM_{1.0}$, $PM_{2.5}$, and PM_{10}.

	$PM_{1.0}$	$PM_{2.5}$	PM_{10}
Mass	13.72 ± 7.72	17.24 ± 8.90	28.37 ± 14.14
NO_3^-	0.71 ± 0.79	1.16 ± 1.08	2.41 ± 1.72
SO_4^{2-}	4.56 ± 3.03	5.40 ± 3.56	5.60 ± 3.39
NH_4^+	1.41 ± 0.67	1.52 ± 0.73	1.57 ± 0.71
OC*	3.16 ± 1.82	3.95 ± 2.50	4.66 ± 2.50
OC1	0.17 ± 0.12	0.19 ± 0.15	0.19 ± 0.12
OC2	0.83 ± 0.38	0.95 ± 0.54	0.99 ± 0.50
OC3	0.76 ± 0.44	0.95 ± 0.56	1.30 ± 0.71
OC4	0.48 ± 0.33	0.71 ± 0.58	0.95 ± 0.62
OP	0.93± 0.74	1.15± 0.83	1.23± 0.78
EC*	1.42 ± 0.76	1.69 ± 1.25	1.69 ± 1.16
EC1	0.96 ± 0.68	1.29 ± 1.16	1.39 ± 1.04
EC2+3	0.46 ± 0.17	0.40 ± 0.18	0.30 ± 0.17

All concentrations are given as mean ± standard deviation in $\mu g\,m^{-3}$.
* OC is the sum of OC1, OC2, OC3, OC4, and OP, and EC is the sum of EC1, EC2, and EC3. See the measurement section for the definition of each sub-component. OC1, OC2, OC3, and OC4 are fractions of OC liberated at different temperatures: 120°, 250°, 450°, and 550°, respectively. Some OC is charred during the gradual increase in temperature and is defined as OP (pyrolyzed organic carbon). EC1, EC2, and EC3 are carbon fractions evolved under an O_2 atmosphere at 550°, 700°, and 800°, respectively, after OC/EC split.

ACPD
11, 20521–20573, 2011

Table 3. Correlation coefficients of absorption and scattering properties of aerosols with EC and sulfate concentrations in $PM_{1.0}$.

	$PM_{1.0}$ EC	$PM_{1.0}$ sulfate
Aethalometer BC (520 nm)[a]	0.94	0.64
Scattering coefficient (550 nm)[b]	0.73	0.79

[a] Aethalometer acquires data at seven wavelengths: 370, 470, 520, 590, 660, 880, and 950 nm.
[b] Nephelometer acquires data at three wavelength: 450, 550, and 700 nm.

ACPD
11, 20521–20573, 2011

Table 4. The ratios of EC1 and EC2+3 concentrations for non-rainy days to those for rainy days in $PM_{1.0}$, $PM_{2.5}$, and PM_{10}.

Non-rainy days (N=31)	$PM_{1.0}$	$PM_{2.5}$	PM_{10}
Rainy days (N=10)			
EC1	1.5	1.8	1.5
EC2+3	1.0	1.1	1.3

ACPD
11, 20521–20573, 2011

Table 5. Meteorological and chemical characteristics of the 5 air mass categories.

	Siberia	Beijing	Shanghai	Yellow Sea	East Sea
Meteorology					
Wind speed ($m\,s^{-1}$)	8.7	7.3	4.6	3.9	3.1
Temperature (°)	11.6	11.8	14.1	14.3	23.8
Relative humidity (%)	56.6	57.5	57.5	76.2	73.4
Gases (ppbv)					
CO	501	648	533	527	613
SO_2	1.7	5.3	5	2	0.5
NO_2	NA[a]	4.9[b]	NA[a]	4.2	4.1
O_3	44.3	46.8	65.1	64.2	41
Particles ($\mu g\,m^{-3}$)					
$PM_{1.0}$					
Mass	7.51	15.16	24.10	22.75	12.29
Nitrate	0.39	0.93	1.83	0.97	0.31
Sulfate	2.01	4.85	9.96	8.70	3.09
TC	3.47	5.96	6.92	5.86	2.99
OC2	0.67	0.95	1.27	1.21	0.72
OP	0.68	1.45	1.44	0.96	0.34
EC1	0.58	1.36	1.78	1.46	0.44
EC2+3	0.40	0.42	0.53	0.76	0.48
PM_{10}					
Mass	23.23	35.90	42.80	40.85	20.87
Nitrate	1.67	3.39	4.31	2.86	1.62
Sulfate	2.84	5.94	11.18	10.72	3.66
TC	4.86	8.35	10.71	7.62	3.82
OC2	0.77	1.17	1.65	1.43	0.77
OP	0.92	1.76	2.10	1.43	0.67
EC1	0.84	1.90	2.93	2.15	0.58
EC2+3	0.21	0.29	0.55	0.44	0.27

[a] NA : Not available.
[b] NA on 14 Feb and 3 Apr.

ACPD
11, 20521–20573, 2011

Table 6. Ratios of major chemical constituents indicating source regions categorized into 5 regimes: Siberia, Beijing, Shanghai, Yellow Sea, and East Sea.

Ratio	$PM_{1.0}$					PM_{10}				
	Siberia	Beijing	Shanghai	Yellow Sea	East Sea	Siberia	Beijing	Shanghai	Yellow Sea	East Sea
OP/Mass	↑	↑	–	–	–	↑	↑	–	–	–
EC1/Mass	↑	↑	–	–	–	↑	↑	↑	–	–
Nitrate/Mass	↑	↑	↑	–	–	–	↑	↑	–	–
Sulfate/Mass	–	–	↑	↑	–	–	–	↑	↑	–
Nitrate/Sulfate	↑	–	–	–	–	↑	↑	–	–	–
OC2/TC	–	–	–	↑	↑	–	–	–	↑	↑
EC2+3/EC1	↑	–	↑	–	↑↑	–	–	↑	–	↑↑
OP/Sulfate	↑↑	↑	–	↓	↓	↑	↑	–	–	–
EC1/Sulfate	↑	↑	–	–	–	↑	↑	–	–	–

The ratios are expressed as symbols: ↑↑ for values larger than mean × 1.5, ↑ for those between mean and mean × 1.5, – for those between mean × 0.5 and mean, and ↓ for those smaller than mean × 0.5.

ACPD
11, 20521–20573, 2011

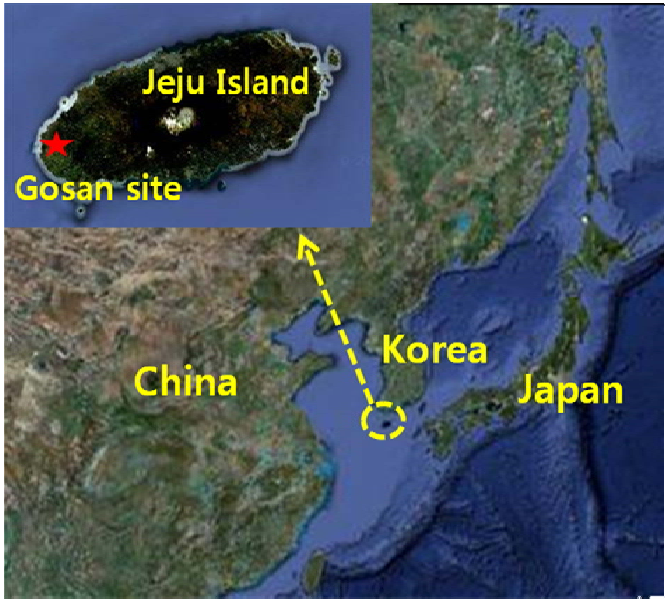

Fig. 1. Map showing Gosan ABC superstation (33.17° N, 126.10° E, 70 m a.s.l.) from Google mapmaker (http://www.google.com/mapmaker). The station is located on the west coast of Jeju Island, South Korea.

ACPD
11, 20521–20573, 2011

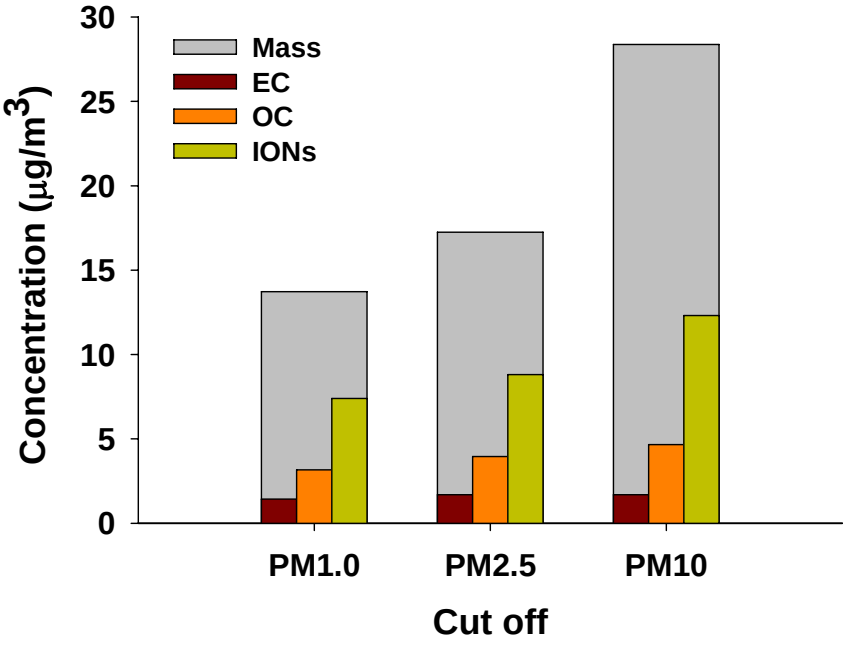

Fig. 2. Mean concentrations of mass, water-soluble ions, EC, and OC in $PM_{1.0}$, $PM_{2.5}$, and PM_{10}. Ions include SO_4^{2-}, NO_3^-, and Cl^- for anions and NH_4^+, K^+, Na^+, Ca^{2+}, and Mg^{2+} for cations.

ACPD
11, 20521–20573, 2011

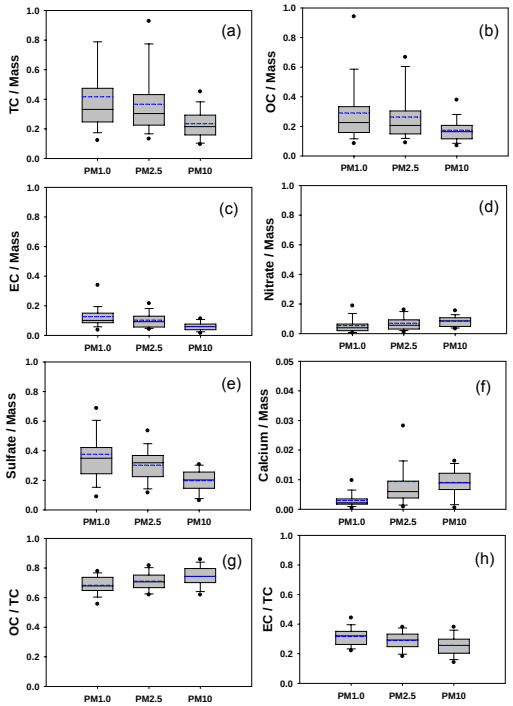

Fig. 3. Ratios of each chemical component to mass or total carbon (TC = OC + EC) in $PM_{1.0}$, $PM_{2.5}$, and PM_{10}: **(a)** total carbon-to-mass, **(b)** OC-to-mass, **(c)** EC-to-mass, **(d)** nitrate-to-mass, **(e)** sulfate-to-mass, **(f)** calcium-to-mass, **(g)** OC-to-TC, **(h)** EC-to-TC, **(i)** OC1-to-TC, **(j)** OC2-to-TC, **(k)** OC3-to-TC, **(l)** OC4-to-TC, **(m)** OP-to-TC, **(n)** EC1-to-TC, **(o)** EC2+3-to-TC. Total Carbon (TC) is the sum of OC and EC, which are the sum of 5 sub-components (OC1, OC2, OC3, OC4, and OP) for OC and 3 components (EC1, EC2, and EC3) for EC (Han et al., 2007; 2010). OP stands for pyrolyzed organic carbon. Solid and blue dotted lines within the box denote the median and the mean value, respectively, and the box represents the 25th and 75th percentiles. Whiskers above and below the box indicate the 90th and 10th percentiles, and solid circles are outliers corresponding to 5th and 95th percentiles of the data.

ACPD
11, 20521–20573, 2011

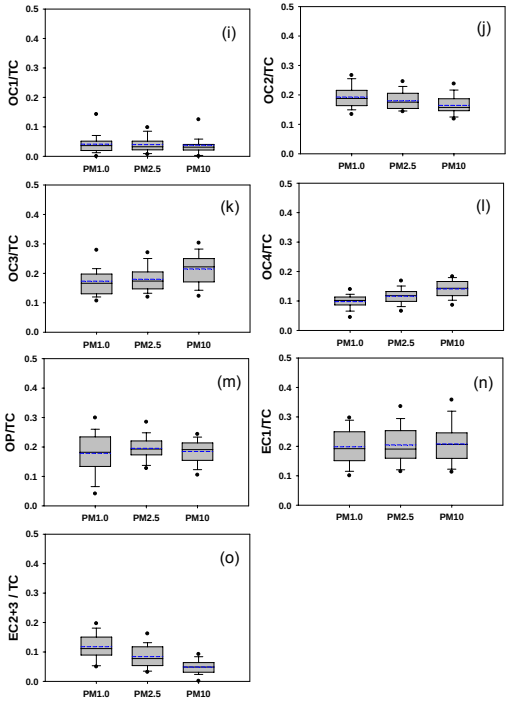

Fig. 3. Continued.

ACPD
11, 20521–20573, 2011

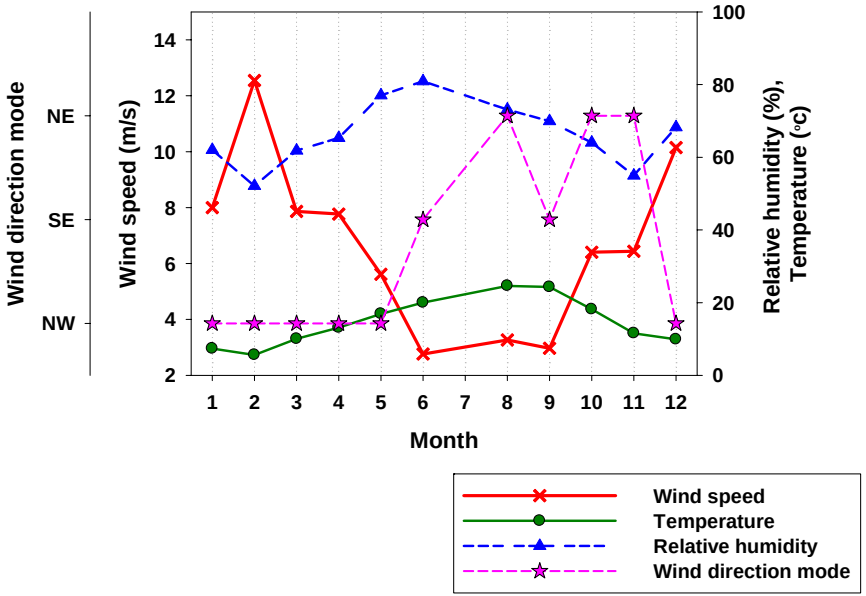

Fig. 4. Monthly variations of meteorological parameters including temperature, relative humidity, wind speed, and wind direction. Wind direction is represented as a mode divided into 8 from N to NW for 1-h data, and the wind mode in this study includes NE, SE, and NW.

ACPD
11, 20521–20573, 2011

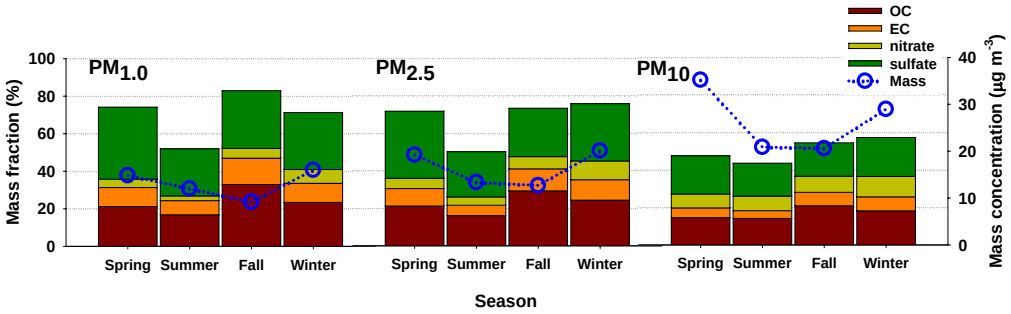

Fig. 5. Seasonal variations of mass concentrations (blue circle) and fractions of OC, EC, nitrate, and sulfate against mass in $PM_{1.0}$, $PM_{2.5}$, and PM_{10}. Spring, summer, fall, and winter include March to May, June to early September, October to November, and December to February, respectively.

ACPD
11, 20521–20573, 2011

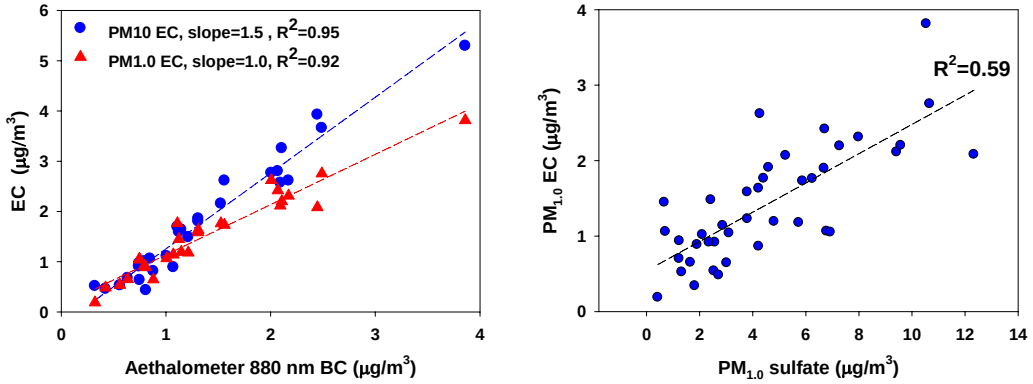

Fig. 6. Correlations of **(a)** BC measured by Aethalometer at 880 nm with EC in $PM_{1.0}$ and PM_{10} and **(b)** sulfate with EC in $PM_{1.0}$. The Aethalometer acquires data at seven wavelengths from the ultraviolet to near-infrared: 370, 470, 520, 590, 660, 880, and 950 nm. BC concentrations were averaged for 24 h in accordance with collection duration for filter samples. The dotted lines represent linear regression fits, for which R^2 values are given.

ACPD
11, 20521–20573, 2011

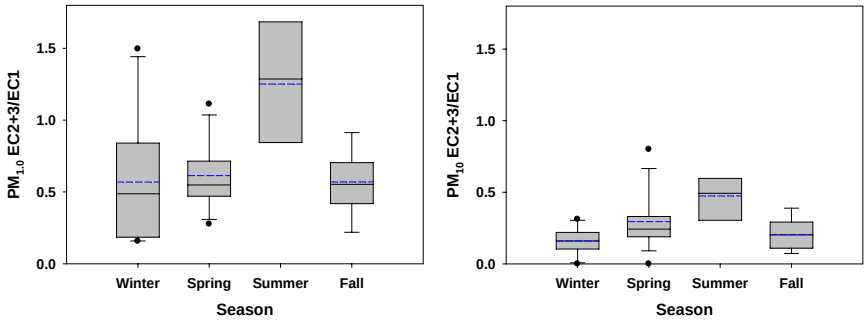

Fig. 7. Seasonal variations of soot-EC to char-EC in $PM_{1.0}$ and PM_{10}. See Fig. 3 for the detailed explanation of box and whisker plot.

ACPD
11, 20521–20573, 2011

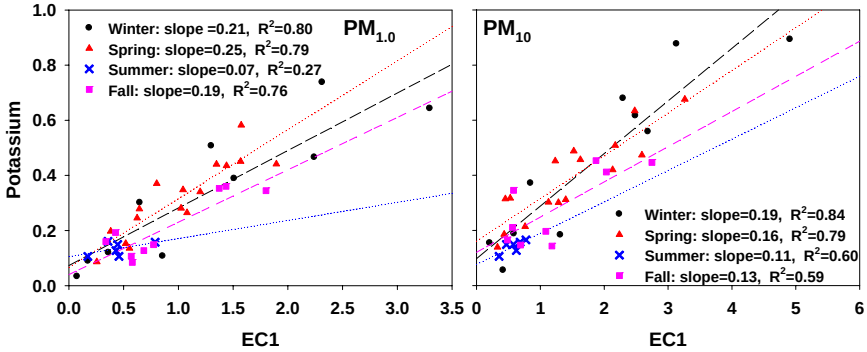

Fig. 8. Correlations of EC1 with potassium for $PM_{1.0}$ and PM_{10} in each season. Lines stand for linear regression fittings, for which slopes and R^2 values are given.

ACPD
11, 20521–20573, 2011

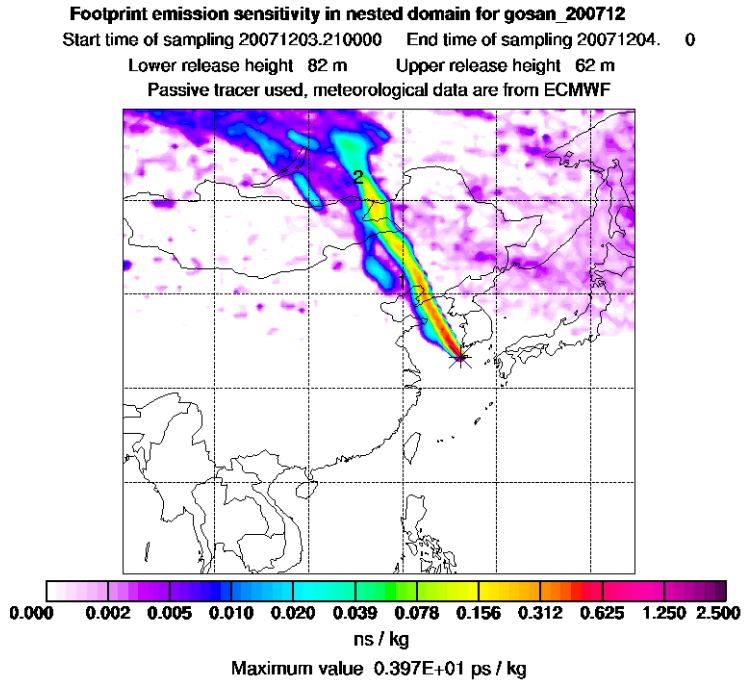

(a)

Fig. 9. Five air mass trajectories representing the influence from **(a)** Siberia region (e.g., 4 December 2007), **(b)** Beijing region (e.g., 3 Januar 2008), **(c)** Shanghai region (e.g., 11 March 2008), **(d)** Yellow Sea region (e.g., 14 April 2008), and **(e)** East Sea region (e.g., 25 August 2008). Backward trajectories were calculated every 3 hours using the Lagrangian particle dispersion model FLEXPART (Stohl et al., 2005; http://zardoz.nilu.no/~andreas/STATIONS/GOSAN/index.html). The model output ($s\,kg^{-1}$) is a potential emission sensitivity distribution of 40 000 particles released in a particular grid cell at the measurement location and during the measurement interval and followed backward in time, which is proportional to the particle residence time in that cell.

ACPD
11, 20521–20573, 2011

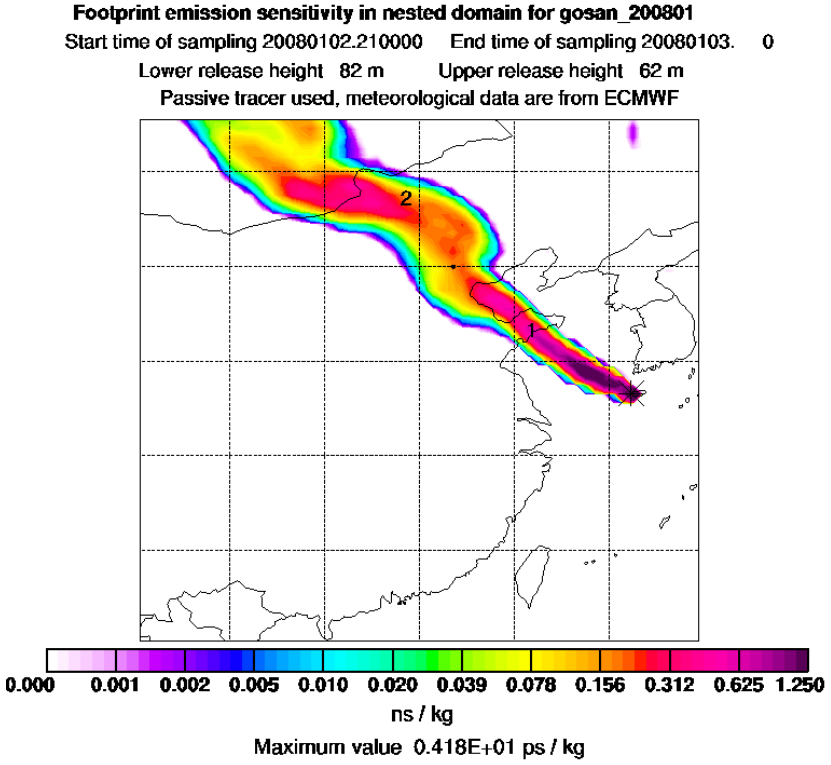

(b)

Fig. 9. Continued.

ACPD
11, 20521–20573, 2011

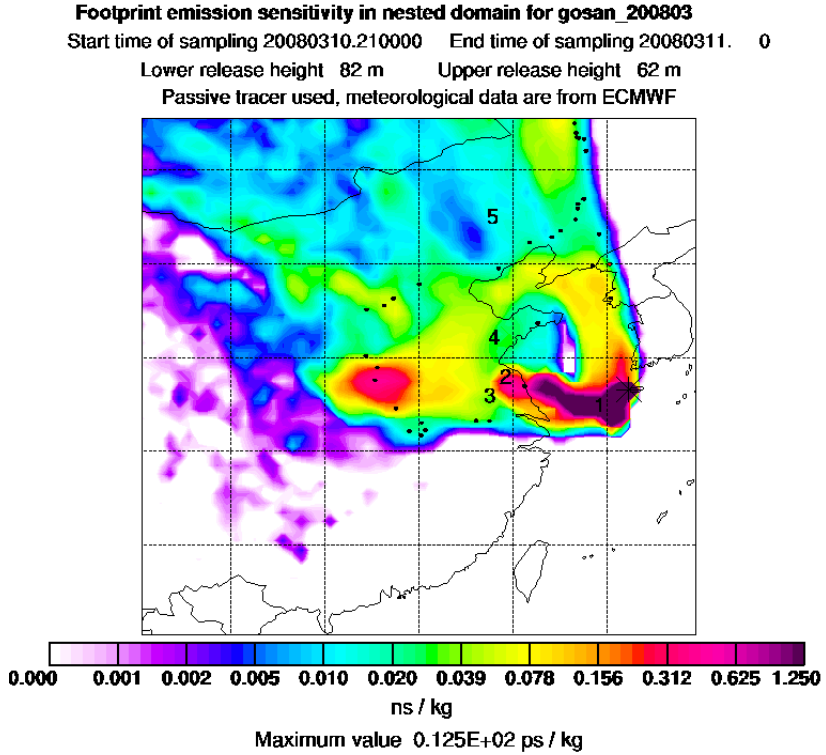

(c)

Fig. 9. Continued.

ACPD
11, 20521–20573, 2011

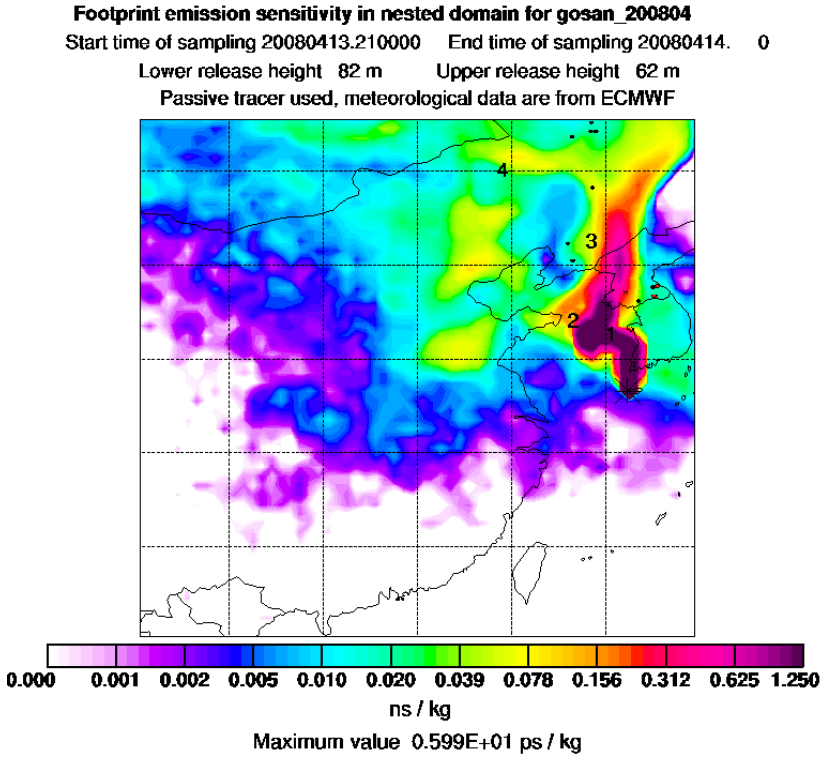

(d)

Fig. 9. Continued.

ACPD
11, 20521–20573, 2011

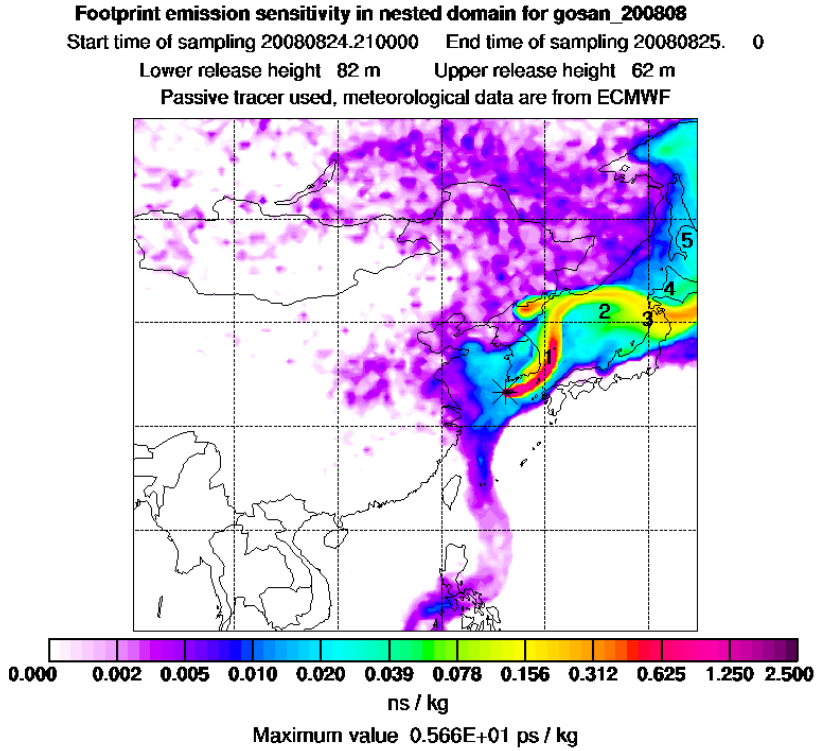

(e)

Fig. 9. Continued.

ACPD
11, 20521–20573, 2011